TOXICOLOGICAL SCIENCES 93(2), 369–381 (2006)
doi:10.1093/toxsci/kfl049
Advance Access publication June 30, 2006

Testicular Gene Expression Profiling following Prepubertal Rat Mono-(2-ethylhexyl) Phthalate Exposure Suggests a Common Initial Genetic Response at Fetal and Prepubertal Ages

Stephanie A. Lahousse, Duncan G. Wallace, Delong Liu, Kevin W. Gaido, and Kamin J. Johnson[1]

Division of Biological Sciences, CIIT Centers for Health Research, Research Triangle Park, North Carolina 27709

Received April 19, 2006; accepted June 23, 2006

Phthalate chemical plasticizers can damage the fetal and postnatal mammalian testis, but several aspects of the injury mechanism remain unknown. Using a genome-wide microarray, the profile of testicular gene expression changes was examined following exposure of postnatal day 28 rats to a single, high dose (1000 mg/kg) of mono-(2-ethylhexyl) phthalate (MEHP). By microarray analysis, approximately 1675 nonredundant genes exhibited significant expression changes; the vast majority were observed at 12 h. Among the 36 genes significantly altered up to the 3-h time point, prominent functional categories were secreted, transcription, and signaling factors. Using quantitative PCR (qPCR), the dose-response of 24 genes was determined after a single MEHP exposure of 10, 100, or 1000 mg/kg. Increasing 114-fold by 12 h at 1000 mg/kg, *Thbs1* (thrombospondin 1) showed the highest level of gene induction. The vast majority of genes analyzed by qPCR exhibited significant expression alterations at the lowest dose level. Interestingly, a unique, dose-dependent expression pattern was observed for the transcription factor *Nr0b1*, steroidogenic genes (*Cyp17a1* and *StAR*), and a cholesterol metabolism gene (*Dhcr7*). For these genes, the direction of expression change at 10 or 100 mg/kg was opposite that observed at 1000 mg/kg. Gene profiling data at 1000 mg/kg MEHP were phenotypically anchored to increased germ cell apoptosis (6 and 12 h) and an interstitial neutrophil infiltrate (12 h). At 10 or 100 mg/kg MEHP, no testicular morphological changes were detected, but a significant increase in germ cell apoptosis was seen at 6 h. Finally, comparison of the prepubertal MEHP microarray data to similar data from fetal dibutyl phthalate (DBP) exposure showed conservation in both the identities of testicular genes altered and the direction of expression changes. For example, 60% of the genes altered within 3 h of prepubertal MEHP exposure also were changed following acute fetal DBP exposure, and the direction of expression change was highly preserved. These data demonstrate that similar genetic targets are altered following fetal and prepubertal phthalate exposure, suggesting that the initial mechanism of fetal and prepubertal phthalate–induced testicular injury is shared.

Key Words: phthalate; testis; gene expression; postnatal; fetal.

Phthalates are industrial chemicals that impart flexibility and resilience to a variety of plastics and consumer goods, including food packaging, medical bags and tubing, and personal care products. Since they are not covalently bound to the product matrix, phthalates can leach from the matrix leading to ubiquitous human exposure (Silva *et al.*, 2004). Several phthalate diester congeners and their monoester metabolites are testicular toxicants in both fetal and prepubertal male rodents (Boekelheide *et al.*, 2004; Liu *et al.*, 2005).

While testicular responses following fetal and prepubertal phthalate exposure show some similarities, significant differences also are observed. Histopathologically, prepubertal and fetal testes both respond initially to high-dose exposure by a collapse of the Sertoli cell vimentin cytoskeleton and a coincident retraction of Sertoli cell processes (Kleymenova *et al.*, 2005; Richburg and Boekelheide, 1996). These changes and others indicate that, at least for prepubertal exposure, the Sertoli cell may be the primary cellular target (Creasy *et al.*, 1983). Long-term histopathological responses between the fetal and prepubertal testis show significant differences. Phthalate-exposed fetal testes fail to correctly organize seminiferous cords and gonocytes coalesce into multinucleated syncytia (Mahood *et al.*, 2005). Ultimately, high-dose fetal exposure produces a highly abnormal postnatal testis characterized by areas of Leydig cell aggregation and dysgenic seminiferous tubules. Apoptosis is not a significant contributing factor to fetal injury (Kleymenova *et al.*, 2005). Unlike fetal exposure, the main prepubertal cellular response following high-dose phthalate exposure is germ cell sloughing into the seminiferous tubule lumen accompanied by extensive germ cell apoptosis (Creasy *et al.*, 1983; Richburg and Boekelheide, 1996). At the molecular level, few studies have examined correlations between fetal and prepubertal phthalate exposure.

The phthalate testicular injury molecular mechanism remains unknown, and because of the significant differences in morphological outcomes, it is unclear if the molecular mechanisms between fetal and prepubertal exposure are similar or unique. We hypothesized that prepubertal phthalate exposure would show time-dependent alterations in testicular gene

[1] To whom correspondence should be addressed at Division of Biological Sciences, CIIT Centers for Health Research, 6 Davis Drive, Research Triangle Park, NC 27709. Fax: (919) 558-1300. E-mail: kjohnson@ciit.org.

expression and that (despite age-dependent phthalate exposure phenotypes) the fetal and prepubertal testicular genetic response would be similar. Here, genome-wide microarray analysis was used to examine testicular gene networks modified in the phthalate-exposed prepubertal rat, and quantitative PCR (qPCR) was employed to determine the phthalate dose-response of select genetic targets. A comparison of the prepubertal and fetal testicular responses showed that similar genetic targets were altered at both ages.

MATERIAL AND METHODS

Animals. Postnatal day (PND) 28 rats were chosen as our model because of its historical use in examination of the postnatal mechanism of phthalate-induced testicular injury and the distinct testicular morphological outcomes at this age compared to fetal phthalate exposure. Male Fisher 344 rats from Charles River Laboratories, Inc (Raleigh, NC) were obtained at PND21. Animals were randomly assigned to a treatment group, with each group containing a minimum of three animals. Animals were housed in the animal facility of the CIIT Centers for Health Research (CIIT, NC), which is accredited by the Association for the Assessment and Accreditation of Laboratory Animal Care International, in a room with controlled humidity and temperature, and HEPA-filtered, mass air-displacement. The room was maintained on a 12:12 light:dark cycle at approximately 22 ± 4°C with a relative humidity of approximately 30–70%. Animals were identified by ear tags and cage cards, and housed three per cage in polycarbonate cages with Alpha-dri cellulose bedding (Shepherd Specialty Papers, Kalamazoo, MI). Rodent diet NIH-07 (Zeigler Brothers, Gardener, PA) and reverse-osmosis water were provided *ad libitum*. This study followed federal guidelines for the care and use of laboratory animals and was approved by the Institutional Animal Care and Use Committee at CIIT.

Because of its historical use in postnatal phthalate mechanistic studies from our laboratory and others, mono-(2-ethylhexyl) phthalate (MEHP) was used for these experiments. Rats were gavaged on PND28 with corn oil vehicle (1 ml/kg; Sigma Chemical Co., St Louis, MO) or MEHP (in corn oil) at 10, 100, or 1000 mg/kg. Purity and concentration of dosing solutions were verified using a Hewlett-Packard 5890 gas chromatograph. Rats were sacrificed 1, 2, 3, 6, or 12 h after dosing by carbon dioxide asphyxiation, and the testes were removed and detunicated. The right testis was placed in RNAlater (Ambion, Inc, Austin, TX) and used for RNA extraction. Following puncture of the tunica albuginea with a 28-gauge needle, the left testis was fixed by overnight immersion in 10% neutral buffered formalin, embedded in paraffin, and used to examine histopathology and measure the germ cell apoptotic index using the terminal deoxy-nucleotidyl transferase-mediated digoxigenin-dUTP nick end labeling (TUNEL) assay.

TUNEL assay. TUNEL was performed on 8-mm testis sections using the ApopTag kit (Oncor, Gaithersburg, MD). Briefly, digoxigenin-dUTP end labeled DNA was detected with anti-digoxigenin-peroxidase antibody followed by peroxidase detection with 0.05% diaminobenzidine and 0.02% H_2O_2. Tissue was counterstained with methyl green. The apoptotic index was determined as described by Richburg and Nanez (2003). At each time point, the slides were blinded, and the number of apoptotic germ cells was counted in 100 randomly selected seminiferous tubules. Only intact, essentially round tubules were counted. The number of tubules having four or more apoptotic germ cells was calculated as a percentage of the total number of tubules examined; this apoptotic index was expressed as average ± SD. Because controls at each time point showed no statistically significant differences, all controls ($n = 17$) were placed into a single group for statistical analyses. The number of statistical units at each time point for the 10, 100, or 1000 mg/kg MEHP groups was 4, 4, and 3, respectively. Using Prism Graphpad 4 software (San Diego, CA), significance between control and treated groups ($p < 0.05$) was determined by one-way ANOVA with a Dunnett's *post hoc* test.

Microarray analysis. Detunicated testes from individual rats were homogenized in RNA Stat-60 reagent (Tel-Test, Friendswood, TX), and RNA was isolated using a RNeasy Maxi Kit (Qiagen, Valencia, CA). RNA integrity was assessed using an Agilent 2100 Bioanalyzer (Agilent Technologies, Palo Alto, CA). Complementary DNA (cDNA) was synthesized from 2 mg of total RNA and purified using the RiboAmp OA 1 Round RNA Amplification kit (Arcturus, Mountain View, CA) according to the manufacturer's protocol. Equal amounts of purified cDNA per sample were used as the template for subsequent *in vitro* transcription reactions for complementary RNA (cRNA) amplification and biotin labeling using the BioArray High Yield RNA Transcript Labeling Kit (Enzo Life Sciences, Inc, Farmingdale, NY). cRNA was purified and fragmented according to the protocol provided with the GeneChip Sample Cleanup Module (Affymetrix, Santa Clara, CA). All GeneChip microarrays (Rat Genome 230 2.0 Array) were hybridized, washed, stained, and scanned using the Complete GeneChip Instrument System according to the Affymetrix Technical Manual. The Rat Genome 230 2.0 microarray contained 31099 probe sets. As on April 2006, analysis of these probe sets using Bioconductor R 2.3.0 software showed that 23250 probe sets were annotated, which mapped to 13,784 unique gene names (Gentleman *et al.*, 2004).

All prepubertal rat microarray primary data have been deposited in the Gene Expression Omnibus (GEO) (http://www.ncbi.nlm.nih.gov/geo/) and are accessible through GEO Series accession number GSE4514. Primary testicular gene expression data for fetal phthalate exposure were obtained from a previous study of rat gestational day 19 exposure to 500 mg/kg dibutyl phthalate (DBP) (Thompson *et al.*, 2005).

To select significantly expressed genes from Affymetrix probe level data, a linear mixed model was used. The perfect-match only data at the probe level was used, and each array was normalized to a common mean on the log2 scale as previously described (Chu *et al.*, 2002). Each probe set was fit to a linear mixed model. The model used was as follows: $y_{ijk} = \mu + T_i + P_j + A_k + \varepsilon_{ijk}$, where y_{ijk} is the normalized log2-transformed perfect-match expression of the ith treatment for the jth probe, μ is the overall mean, T_i is the effect of the ith treatment, P_j is the effect of the jth probe, A_k is the effect of the kth chip, and ε_{ijk} is the residual. The A_k's and ε_{ijk}'s are assumed to be independent, and normally distributed, e.g., $N(0, \sigma_a^2)$, and $N(0, \sigma^2)$. The treatment and probe effects were fixed and the array A_k's were assumed to be random effects. The parameters for the fixed and random effects were estimated using restricted maximum likelihood. Selected genes demonstrated significant changes in expression level following treatment when compared to controls using mixed-model F-tests. The Bonferroni method was used to identify genes with a significance level of 5% from each individual comparison of treatment versus control. SAS Microarray Solution version 1.3 software (Cary, NC) was used to compute the results.

Gene networks were generated using Ingenuity Pathways Analysis software (Ingenuity Systems, Redwood City, CA). A gene network is a graphical representation of the molecular relationships between genes or gene products. Within a network, genes or gene products are represented as nodes, and the biological relationship between two nodes is represented as an edge (line). Nodes are displayed using various shapes that represent the functional class of the gene product. Edges are displayed as various line types that describe the nature of the relationship between the nodes; solid lines are direct interactions while dashed lines represent indirect interactions. Edges are substantiated by at least one reference from the literature, a textbook, or canonical information stored in the Ingenuity Pathways Knowledge Base. The intensity of the node color indicates the level of up- (yellow) or down- (blue) regulation, as determined by microarray analysis.

The qPCR. Total RNA was isolated from the detunicated testis of control and treated animals using the RNeasy Maxi Kit (Qiagen) following the manufacturer's protocol. The number of animals within each group was controls ($n = 11$); 10 and 100 mg/kg ($n = 4$); and 1000 mg/kg ($n = 3$ or 4). Subsequent reverse transcription reactions, quality control for reverse transcriptase reactions, and qPCR reactions were performed as described (Lehmann *et al.*, 2004). As a template, cDNA prepared from detunicated PND28 testes was used. For the cDNA reaction, samples containing 1 mg of RNA were reverse transcribed using the TaqMan Reverse Transcription kit (Applied Biosystems,

TABLE 1
qPCR Taqman Assays

Gene	Taqman assay[a]
Ctgf	Rn00573960_g1
Cx3cl1	Rn00593186_m1
Cxcl10	Rn00594648_m1
Cyp17a1	Rn00594648_m1
Dhcr7	Rn00574366_m1
Dusp6	Rn00518185_m1
Edn1	Rn00561129_m1
Egr1	Rn00561138_m1
Junb	Rn00572994_s1
Ier3	Rn01531989_g1
Il1a	Rn00566700_m1
Map3k8	Rn00587750_m1
Nfkb1	Rn01399583_m1
Nfkb2	Rn01413849_g1
Nr0b1	Rn00584062_m1
Nr4a1	Rn00577766_m1
StAR	Rn00580695_m1
Stat3	Rn00562562_m1
Stc1	Rn00579636_m1
Stc2	Rn00573702_m1
Thbs1	Rn01513688_g1
Tnfrsf1a	Rn00565310_m1
Tnfrsf12a	Rn00710373_m1
Tnfrsf6	Rn00594913_m1

[a]Applied Biosystems assay number.

Foster City, CA) and random hexamer primers. PCR amplifications were performed in 20 ml reactions containing 40 ng of template DNA, 1× volume of prevalidated TaqMan Gene Expression Assay mix for each gene (Table 1), and a 1× volume of TaqMan Universal PCR Master Mix. The amplification protocol used was as follows: initial 10-min denaturation at 95°C followed by 40 cycles of 95°C for 15 s and 60°C for 1 min. Amplification signals were detected continuously with an Applied Biosystems 7700 Real-Time PCR system.

For some genes, qPCR was performed using a TaqMan Low Density Array (LDA) preloaded with prevalidated TaqMan gene expression assays (Applied Biosystems). For this assay, 100 ng of cDNA was combined with 47.5 ml RNase/DNase free water and 50 µl TaqMan Universal PCR Master Mix for a total volume of 100 ml and loaded into the fill ports of the TaqMan array. The LDA was centrifuged briefly to load the sample-specific reaction mixes into the individual wells, sealed, and loaded into a 7900 HT Real-Time PCR system (Applied Biosystems). The amplification protocol was as follows: initial 2-min incubation at 50°C and 10-min denaturation at 95°C followed by 40 cycles of 95°C for 15 s and 60°C for 1 min.

Analysis of the qPCR data was conducted using the equation set forth by Pfaffl (2001), in which efficiencies were used for both the gene of interest and the calibrator (glyceraldehyde-3-phosphate dehydrogenase or 18-s ribosomal RNA). The average C_t of samples run in duplicate or triplicate was used to establish expression relative to the calibrator. Significance ($p < 0.05$) of the qPCR data was determined by one-way ANOVA and a Dunnett's *post hoc* test.

RESULTS

Testicular Germ Cell Apoptosis and Neutrophil Infiltration following MEHP Exposure

Germ cell apoptosis following high-dose phthalate exposure of prepubertal rats is documented (Richburg and Boekelheide, 1996), and a testicular interstitial neutrophil infiltrate has been observed occasionally (Creasy *et al.*, 1983). To compare our phthalate exposure outcome with previous studies and phenotypically anchor the testicular gene expression analyses, germ cell apoptosis and interstitial histology was analyzed. In vehicle-exposed animals, 10% of seminiferous tubules displayed four or more apoptotic germ cells (Fig. 1). At 1, 2, or 3 h following 1000 mg/kg MEHP exposure, no significant change in germ cell apoptosis was seen. Similar to previous observations by others (Richburg and Boekelheide, 1996), a significant increase in germ cell apoptosis was noted at 6 and 12 h. To determine if lower MEHP dose levels produced a similar response, germ cell apoptosis was examined at 6 or 12 h

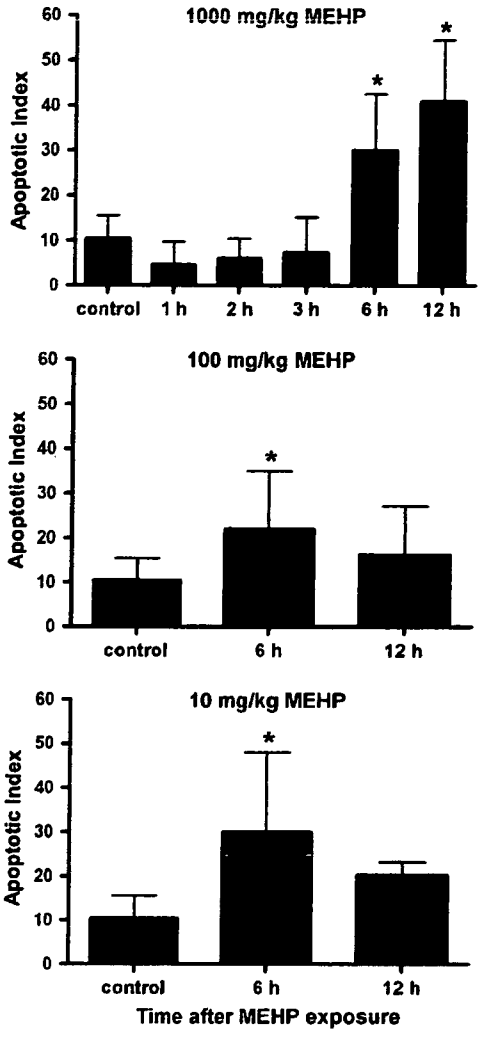

FIG. 1. Germ cell apoptotic levels following prepubertal MEHP exposure. A germ cell apoptotic index based upon quantifying TUNEL-positive germ cells was determined at various time points following a single 1000, 100, or 10 mg/kg MEHP exposure. Each MEHP exposure time-point group was compared statistically to the control group using a one-way ANOVA and Dunnett's *post hoc* test. *$p < 0.05$. Data are shown as mean ± SD.

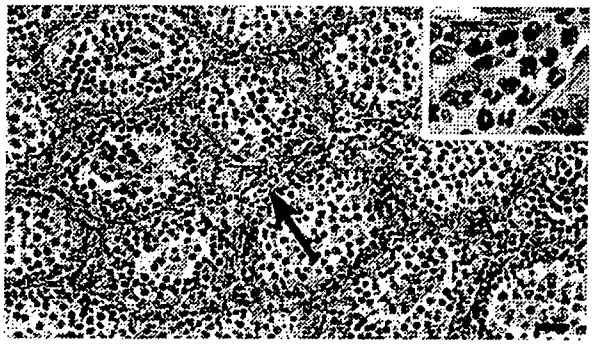

FIG. 2. Interstitial lymphocytic infiltrate after prepubertal MEHP exposure. This image shows a 12-h 1000 mg/kg MEHP-exposed prepubertal testis paraffin section stained with hematoxylin and eosin. A prominent infiltration of polymorphonuclear cells (neutrophils) into the interstitium was observed (arrow). A higher magnification image of the interstitial infiltrate is shown in the inset. Bar = 50 μ.

following a single 10 or 100 mg/kg MEHP exposure. At both dose levels, germ cell TUNEL staining was significantly increased at the 6 h time point (Fig. 1). As for a testicular inflammatory response following MEHP exposure, two out of three animals at the 12-h time point (1000 mg/kg) contained a prominent interstitial lymphocytic infiltration. This infiltrate appeared to be composed mainly of neutrophils (polymorphonuclear cells) (Fig. 2) and was not observed in testes of animals from the other treatment groups or the vehicle control group (data not shown). Apart from increased apoptosis, no change in testicular histopathology following 10 or 100 mg/kg MEHP was detected (data not shown).

Prepubertal Testis Gene Profile following Acute Phthalate Exposure

Using genome-wide Affymetrix microarrays, changes in prepubertal testis gene expression were monitored 1, 2, 3, 6, and 12 h following exposure to 1000 mg/kg MEHP. Of the nearly 23,000 annotated probe sets present on the microarray, approximately 1675 displayed a significant expression change within 12 h of MEHP exposure (Supplementary Table 1). Although more than 1675 Affymetrix probe sets were altered, about 10% were duplicate probe sets that corresponded to a single gene based upon assigned or determined gene identity. For numerical analysis purposes, duplicate genes were culled. The stringent statistical method employed to examine the microarray data resulted in no genes showing significantly altered expression at the 1-h time point. However, expression of the immediate early transcription factors *Egr1* and *Fos* were induced at this time nearly 3- and 1.5-fold, respectively (Table 2). By 2 h after exposure, 26 genes were changed, and all genes displayed an expression increase. At 3, 6, and 12 h, the number of new genes that became significantly altered was 10, 51, and approximately 1595, respectively. Although the large number of gene changes observed at 12 h correlated with a neutrophil infiltrate, it remained uncertain which gene changes solely reflected infiltration of this new cell population. Typically, genes altered in response to the 1000 mg/kg MEHP exposure remained affected through the 12 h time point. The 6 h time point was the first period in which a reduction in gene expression was observed; in general, genes showing reduced expression following phthalate exposure were involved in metabolic processes.

Significantly changed genes (by microarray analysis) within 6 h of exposure were categorized into general functional groups. Categorization was derived from the Affymetrix website (http://www.affymetrix.com) or a target sequence homology basic local assignment search tool search to identify the gene followed by a Pubmed literature search. The majority of altered genes at 3 h of MEHP exposure were modulators of intracellular signal transduction, extracellular interactions, or gene transcription (Table 3). Additional functional classifications included genes encoding transmembrane or cytoskeletal proteins and those involved in metabolism or response to stress. By 6 h, signal transduction and transcriptional categories remained prominent but a larger number of genes encoding metabolic factors also responded.

Many of the genes showing the earliest alterations were members of the immediate early response gene family that may regulate NF-κB signaling or downstream targets of NF-κB transcriptional activity. Immediate early response genes included *Cyr61*, *Ctgf*, *Dusp1*, *5*, and *6*, *Egr1*, *Ier3*, *Jun*, and *Junb*. At 2 h, activation of the NF-κB pathway was suggested by an increase in two genes that are downstream targets of NF-κB signaling (*Nfkbia* and *Tnfaip3*) (Heyninck and Beyaert, 2005). An additional gene encoding a modulator of NF-κB activity (*Nfkbiz*) and a subunit of the NF-κB transcriptional complex (*Nfkb2*) were induced within 6 h.

Among the testicular genes induced within 6 h of prepubertal MEHP exposure were several encoding secreted proteins. This group consisted of chemokines (*Cxcl1* and *Cxcl10*), a pro-inflammatory cytokine (*Il1a*), and matricellular proteins (*Cyr61*, *Ctgf*, and *Thbs1*). At 12 h, expression of receptors for these secreted ligands also was stimulated significantly. For example, several integrin receptor genes for the secreted matricellular proteins were induced such as *Itgav*, *Itgb1*, and *Itga6* (Chen *et al.*, 2000; Lau and Lam, 2005). *Sdc4*, encoding the Cyr61 receptor syndecan-4 (Todorovicc *et al.*, 2005), was increased over fourfold by 12 h.

A plethora of genes potentially mediating MEHP-induced germ cell apoptosis were altered. Some of the significantly induced genes at the 2- and 3-h time points have been associated with apoptosis in various models. Within this list were *Thbs1* (Friedl *et al.*, 2002), *Edn1* (Cai *et al.*, 2000), *Ctgf* (Moussad and Brigstock, 2000), *Cyr61* (Todorovicc *et al.*, 2005), *Ier3* (Kruse *et al.*, 2005), *Atf3* (Lu *et al.*, 2006), *Egr1* (Kim *et al.*, 2006), *Egr3* (Xi and Kersh, 2004), and genes encoding components of the activating protein 1 transcriptional complex (*Fos*, *Jun*, and *Junb*) (Hess *et al.*, 2004). Concomitant with an increase in

TABLE 2
Genes Significantly Altered through 6 h following Prepubertal 1000 mg/kg MEHP Exposure

		Fold change (log2 scale)[a]					−log10 (p value)[a,b]				
Affymetrix ID	Gene	1 h	2 h	3 h	6 h	12 h	1 h	2 h	3 h	6 h	12 h
1375781_at	—	0.10	**0.49**	0.19	0.08	−0.11	0.62	**7.37**	1.48	0.43	0.71
1380306_at	—	−0.16	**0.67**	0.35	0.34	−0.15	0.84	**8.03**	2.76	2.61	0.75
1397225_at	—	−0.04	**0.42**	0.21	0.23	−0.08	0.28	**8.31**	2.56	2.92	0.57
1376066_at	Arhe	0.00	**0.35**	0.42	0.36	0.48	0.00	**7.81**	10.58	8.16	13.39
1386994_at	Btg2	0.10	**0.77**	0.60	0.98	1.45	0.33	**6.68**	4.36	10.05	18.99
1387316_at	Cxcl1	0.09	**1.72**	1.61	2.16	3.17	0.19	**16.32**	14.59	23.36	40.17
1368290_at	Cyr61	0.22	**1.13**	1.17	1.42	1.97	1.49	**21.75**	22.93	30.75	47.27
1368124_at	Dusp5	0.03	**0.91**	0.73	1.21	1.11	0.08	**7.80**	5.38	12.64	10.95
1377064_at	Dusp6	−0.03	**0.63**	0.42	0.44	0.91	0.08	**6.79**	3.33	3.62	12.41
1369519_at	Edn1	0.06	**0.65**	0.81	0.81	1.11	0.23	**7.12**	10.38	10.35	17.29
1368321_at	Egr1	1.46	**2.56**	1.61	2.08	2.41	5.37	**13.89**	6.36	9.81	12.56
1369182_at	F3	0.17	**0.45**	0.22	0.26	0.59	2.48	**12.15**	3.63	4.79	18.65
1388587_at	Ier3	0.20	**1.38**	1.16	1.45	1.95	0.74	**17.01**	12.81	18.40	28.84
1371170_a_at	Il1a	0.01	**0.63**	0.61	0.96	1.25	0.03	**7.91**	7.37	15.88	23.99
1369788_s_at	Jun	0.10	**0.63**	0.48	0.77	0.92	0.47	**7.93**	5.10	11.27	15.12
1387788_at	Junb	0.09	**0.49**	0.44	0.57	1.34	0.49	**7.06**	6.02	9.30	35.14
1389538_at	Nfkbia	0.05	**0.52**	0.46	0.49	0.63	0.36	**11.64**	9.31	10.41	15.87
1370174_at	Ppp1r15a	0.08	**0.52**	0.46	0.72	0.87	0.50	**9.02**	7.41	15.63	21.19
1384148_at	Rab20_predicted	−0.03	**0.63**	0.64	0.85	1.26	0.10	**7.04**	7.39	11.82	22.18
1374176_at	RGD1308059	−0.06	**0.36**	0.08	0.04	0.00	0.83	**14.16**	1.13	0.41	0.04
1389199_at	Ab2-095_similar	0.06	**0.60**	0.52	0.57	1.02	0.26	**8.04**	6.26	7.23	18.94
1381246_at	Phf21b_similar	0.02	**0.38**	0.32	0.51	0.30	0.10	**8.94**	6.69	14.99	5.98
1392529_at	Spry4_predicted	0.08	**0.34**	0.27	0.26	0.77	0.69	**7.33**	4.84	4.50	26.82
1393559_at	Stc1	−0.06	**1.03**	0.85	0.53	0.73	0.12	**7.83**	5.67	2.55	4.34
1385641_at	Tnfaip3	0.03	**0.53**	0.56	0.53	1.05	0.14	**11.98**	12.90	11.97	34.19
1392613_at	Zbtb16	−0.01	**0.53**	0.20	0.32	−0.04	0.08	**14.31**	2.70	6.00	0.29
1379437_at	B3galtl	−0.04	0.13	**0.54**	0.51	0.08	0.20	0.76	**7.55**	6.72	0.39
1367631_at	Ctgf	0.20	0.51	**1.73**	2.07	2.02	0.59	2.28	**17.56**	23.33	22.48
1387969_at	Cxcl10	0.00	0.44	**0.54**	0.62	1.41	0.01	4.88	**6.93**	8.98	32.57
1368146_at	Dusp1	0.25	0.51	**0.86**	1.10	1.46	1.55	4.99	**11.83**	17.71	27.52
1370542_a_at	Elf1	−0.07	0.06	**0.43**	0.17	0.57	0.44	0.39	**7.74**	1.65	12.35
1369118_a_at	Gnrhr	−0.04	0.16	**0.41**	0.09	0.10	0.28	1.75	**8.02**	0.67	0.90
1368075_at	Lipa	0.01	0.24	**0.35**	0.36	0.24	0.05	4.82	**9.02**	9.71	4.97
1374816_at	RGD1359197	−0.04	0.15	**0.44**	0.53	0.30	0.23	1.25	**7.39**	9.86	3.78
1381390_at	RGD1311768	0.04	0.17	**0.34**	0.42	0.07	0.29	2.35	**7.47**	10.63	0.58
1379936_at	Tpm1	0.11	0.28	**0.49**	0.44	0.49	0.68	2.72	**7.14**	5.93	6.99
1372490_at	—	0.04	−0.03	−0.04	**−0.24**	−0.23	0.47	0.25	0.40	**6.62**	6.26
1372539_at	—	0.06	0.01	0.02	**−0.25**	−0.29	0.62	0.08	0.20	**6.71**	8.65
1378090_at	—	−0.02	−0.05	−0.06	**−0.34**	−0.42	0.15	0.47	0.61	**9.11**	12.83
1378561_at	—	0.00	0.07	0.06	**0.19**	−0.03	0.05	1.37	1.10	**7.16**	0.35
1378593_at	—	−0.01	0.47	0.45	**0.59**	0.35	0.03	4.44	4.07	**6.60**	2.68
1378754_at	—	−0.03	0.08	0.13	**0.42**	0.87	0.15	0.51	1.00	**7.05**	23.23
1378778_a_at	—	0.02	0.13	0.34	**0.54**	0.71	0.07	0.68	3.12	**6.86**	10.85
1382031_at	—	−0.02	0.10	0.07	**0.44**	−0.18	0.16	1.46	0.95	**16.99**	3.87
1392971_at	—	−0.02	0.21	0.43	**0.76**	0.56	0.05	0.91	2.83	**7.37**	4.38
1393303_at	—	−0.11	−0.13	−0.07	**−0.23**	0.03	2.82	3.56	1.18	**9.23**	0.46
1397577_at	—	−0.10	−0.14	−0.03	**−0.21**	0.02	2.40	4.07	0.39	**8.80**	0.27
1369268_at	Atf3	0.05	0.38	0.37	**0.99**	1.75	0.11	1.79	1.70	**8.69**	21.95
1379368_at	Bcl6	0.07	0.30	0.22	**0.40**	0.78	0.52	4.53	2.63	**7.41**	21.94
1367755_at	Cdo1	−0.04	−0.04	0.17	**0.54**	1.02	0.17	0.15	1.15	**7.77**	22.24
1398591_at	Ccrl2	0.01	0.13	0.29	**0.41**	0.32	0.07	1.72	6.42	**11.07**	7.54
1384837_at	Cd69	0.01	0.05	0.12	**0.18**	0.15	0.12	0.91	3.03	**6.65**	4.91
1370245_at	Ctsl	0.02	0.25	0.34	**0.66**	1.10	0.05	1.35	2.18	**6.64**	15.83
1368189_at	Dhcr7	−0.04	−0.05	−0.20	**−0.55**	−1.03	0.19	0.25	1.75	**9.43**	25.89
1383353_at	Efnb2_homolog	−0.01	−0.09	−0.26	**−0.37**	−0.66	0.05	0.86	4.89	**8.78**	22.35
1392791_at	Egr3	0.21	1.18	0.70	**1.39**	2.35	0.44	5.95	2.46	**7.85**	18.71

TABLE 2—*Continued*

Affymetrix ID	Gene	Fold change (log2 scale)[a]					−log10 (*p* value)[a,b]				
		1 h	2 h	3 h	6 h	12 h	1 h	2 h	3 h	6 h	12 h
1387442_at	Egr4	0.01	0.39	0.40	**0.72**	0.23	0.02	3.28	3.46	**9.30**	1.38
1377635_at	Fmo2	−0.06	0.00	0.10	**0.25**	−0.08	0.81	0.01	1.83	**8.35**	1.14
1368304_at	Fmo3	−0.04	0.12	0.19	**0.38**	−0.06	0.22	1.06	2.07	**6.72**	0.37
1375043_at	Fos	0.57	1.48	0.81	**1.73**	2.57	1.29	6.01	2.21	**7.82**	15.22
1373122_at	Jub	0.06	0.08	0.28	**0.40**	0.50	0.41	0.60	3.94	**7.42**	10.71
1387264_at	Kcnk6	0.01	0.30	0.36	**0.55**	0.45	0.04	3.53	4.90	**10.13**	7.14
1397897_x_at	LOC314860	0.02	0.08	0.10	**0.29**	−0.01	0.19	1.04	1.34	**8.22**	0.08
1383490_at	LOC315163	−0.02	−0.01	−0.09	**−0.41**	−0.70	0.10	0.06	0.70	**8.36**	20.54
1390790_a_at	LOC361349	−0.07	−0.01	−0.24	**−0.60**	−0.33	0.33	0.05	1.66	**7.81**	2.87
1393696_at	LOC499856	−0.01	0.02	0.08	**0.50**	0.21	0.09	0.18	0.96	**17.77**	4.07
1380229_at	Maff	−0.04	0.16	0.31	**0.43**	1.23	0.20	1.45	4.45	**7.81**	39.87
1372211_at	Mafk	0.01	0.24	0.29	**0.34**	0.51	0.06	3.70	5.09	**6.58**	12.94
1395172_at	Map1b	−0.02	0.06	0.14	**0.31**	0.48	0.15	0.56	1.88	**6.93**	14.11
1397579_x_at	MGC94198	0.09	0.01	−0.20	**−0.34**	−0.48	0.89	0.10	3.26	**7.93**	14.21
1380321_at	Mtus1	−0.01	0.12	0.27	**0.30**	0.17	0.09	1.55	5.98	**7.24**	2.87
1376648_at	Mycn	−0.09	−0.15	−0.12	**−0.42**	−0.34	0.61	1.30	0.93	**7.42**	5.12
1375989_a_at	Nfkb2	−0.02	0.05	0.30	**0.52**	1.29	0.07	0.24	2.95	**7.34**	31.00
1378032_at	Nfkbiz_predicted	0.02	0.51	0.49	**1.01**	1.72	0.08	6.30	6.03	**19.88**	42.49
1370530_a_at	Pld1	0.00	0.14	0.22	**0.34**	0.58	0.00	2.18	5.05	**10.33**	24.08
1388103_at	Prl	−0.02	0.10	0.21	**0.35**	0.40	0.11	0.92	3.02	**7.08**	9.15
1375020_at	Rin3	−0.02	0.04	0.18	**0.33**	0.50	0.14	0.29	2.69	**6.97**	14.42
1381533_at	Rnd1	0.04	0.31	0.38	**0.58**	1.53	0.21	3.47	4.82	**9.77**	43.28
1397620_at	Sh3md2	0.04	0.13	0.16	**0.29**	0.16	0.37	1.93	2.60	**7.19**	2.75
1377975_at	Cdk5r1_similar	−0.04	0.21	0.23	**0.36**	0.13	0.37	4.64	5.16	**11.48**	2.13
1372681_at	Stxbp6	0.02	−0.01	0.13	**0.52**	0.66	0.06	0.02	0.81	**7.33**	10.68
1379960_at	Susd3	−0.01	−0.20	−0.15	**−0.50**	−0.73	0.07	1.85	1.19	**8.48**	16.04
1374529_at	Thbs1	0.01	0.46	0.85	**1.54**	3.31	0.01	1.22	3.18	**8.72**	29.46
1388497_at	Them2	−0.12	−0.09	−0.09	**−0.22**	−0.37	2.56	1.58	1.63	**7.33**	17.52
1386162_at	Txk	−0.01	0.08	0.21	**0.25**	0.17	0.07	1.12	5.30	**7.13**	3.48
1393140_at	Zc3h12a	0.02	0.09	0.11	**0.28**	0.43	0.16	1.32	1.76	**8.75**	18.12
1387870_at	Zfp36	0.17	0.44	0.51	**0.73**	1.61	0.67	2.93	3.75	**6.85**	24.75

[a]Values in bold represent the initial time point at which expression changes became statistically significant.
[b]Values shown are unadjusted. The cutoff *p* value ($10^{-6.49}$) corresponds to a justified *p* value of 0.05.

TUNEL-positive germ cells, genes associated with apoptosis induction via either the c-Jun N-terminal kinase (JNK)–stimulated intrinsic (mitochondrial) pathway or the tumor necrosis factor receptor (TNFR) family–mediated extrinsic pathway were increased. Within the JNK apoptotic pathway, MEHP increased expression of genes encoding a JNK-activating scaffolding protein (*Sh3md2*), a JNK kinase (*Map2k4*), and a negative regulator of Map2k4 activity (*Gadd45b*) (Kukekov *et al.*, 2006; Papa *et al.*, 2004). At 12 h, multiple components of the TNFR apoptotic pathway displayed significantly altered expression: *Cflar*, *Cradd*, *Ripk1*, *Ripk2*, *Ripk3*, *Tnfrsf1a*, *Tnfrsf6*, *Tnfrsf21*, *Tnf*, and *Tradd*. Caspases, the main executioners of apoptosis, showed significant increases after cell death began; induction of *Casp3*, *11*, and *12* was detected beginning at 12 h.

A deficit in testicular steroidogenesis is a prominent outcome of fetal rat phthalate exposure. While the prepubertal rat testis is less sensitive than the fetal testis regarding phthalate-induced decreases in testosterone levels (Akingbemi *et al.*, 2001; Lehmann *et al.*, 2004), the gene encoding p450 side chain cleavage (*Cyp17a1*) declined 85% by 12 h and *Hsd3b1* was decreased 60% (Supplementary Table 1) after exposure to 1000 mg/kg MEHP. Although not significant by microarray analysis, *StAR* mRNA levels were reduced after 6 h at this dose level (see below). In addition to these steroidogenic genes, other factors known to modulate Leydig cell androgen production *in vivo* or *in vitro* showed altered expression. Among this list were the transcription factors *Nr4a1* and *Nr0b1*, a cholesterol-modifying gene (*Ch25h*), and the secreted factors *Tnf*, *Il1a*, *Il1b*, and *Wnt4* (Hales, 2002; Jo and Stocco, 2004; Jordan *et al.*, 2003; Lukyanenko *et al.*, 2001).

Dose Response of Selected Genes Analyzed by qPCR

To validate the microarray results and identify genes altered at lower doses of MEHP, the expression of 24 genes was examined by Taqman qPCR after acute exposure to MEHP at dose levels of 10, 100, or 1000 mg/kg. The genes chosen for this

TABLE 3
Functional Categorization of Genes Significantly Altered up to 3 h after Prepubertal 1000 mg/kg MEHP Exposure[a]

Gene	Affymetrix ID	Functional category
Arhe	1376066_at	Signal transducer activity
Dusp1	1368146_at	Signal transducer activity
Dusp5	1368124_at	Signal transducer activity
Dusp6	1377064_at	Signal transducer activity
Nfkbia	1389518_at	Signal transducer activity
Rab20_predicted	1384148_at	Signal transducer activity
Spry4_homolog	1392529_at	Signal transducer activity
Tnfaip3	1385641_at	Signal transducer activity
Ctgf	1367631_at	Extracellular region
Cxcl1	1387316_at	Extracellular region
Cxcl10	1387969_at	Extracellular region
Cyr61	1368290_at	Extracellular region
Edn1	1369519_at	Extracellular region
Il1a	1371170_a_at	Extracellular region
Stc1	1393559_at	Extracellular region
Egr1	1368321_at	Transcription regulator activity
Elf1	1370542_a_at	Transcription regulator activity
Jun	1369788_s_at	Transcription regulator activity
Jimb	1387785_at	Transcription regulator activity
Phf21b_similar	1381246_at	Transcription regulator activity
Zbtb16_predicted	1392613_at	Transcription regulator activity
F3	1369182_at	Integral to membrane
Gnrhr	1369113_a_at	Integral to membrane
B3galt1_predicted	1379437_at	Metabolism
Lipa	1368075_at	Metabolism
Btg2	1386994_at	Response to stress
Ier3	1388587_at	Response to stress
Ppp1r15a	1370174_at	Response to stress
RGD1359197	1374816_at	Cytoskeletal
Tpm1	1379936_at	Cytoskeletal
—	1375781_at	Unknown
—	1380306_at	Unknown
—	1397225_at	Unknown
Similar to Ab2-095	1389199_at	Unknown
RGD1308059	1374176_at	Unknown
RGD1311768	1381390_at	Unknown

[a]Genes shaded in gray showed significant expression changes via microarray analysis in the fetal rat testis within 18 h of 500 mg/kg DBP exposure.

analysis represented a wide spectrum of cellular pathways and processes. Nearly all genes examined by qPCR showed significant expression changes in the microarray analysis prior to observation of a testicular neutrophil infiltrate. In addition, genes regulating phthalate-induced decreases in fetal steroidogenesis (*StAR*) and prepubertal germ cell apoptosis (*Tnfrsf6*) also were analyzed (Lehmann *et al.*, 2004; Richburg *et al.*, 2000).

Overall, the high-dose qPCR data validated the high-dose microarray results, and all genes showed significant expression changes at 10 and/or 100 mg/kg MEHP. In the microarray experiment, a trend of altered expression was noted for numerous genes several hours prior to the differential becoming statistically significant; this earlier trend often became statistically significant using qPCR. Three general observations were noted in the qPCR data: (1) compared to microarray data, the qPCR fold change was higher consistently, which likely reflects different normalization procedures; (2) unlike the 1000-mg/kg dose level, exposure to 100 mg/kg MEHP produced a transient expression change in many genes that were resolved by 12 h following exposure; and (3) compared to higher dose levels, exposure to 10 mg/kg MEHP produced a several hour delayed response. All genes showed altered expression at the 100- and 1000-mg/kg dose levels, and 21 out of the 24 genes were changed at 10 mg/kg. Among the genes examined, the largest expression increase was observed for *Thbs1* (encoding thrombospondin 1; Tbs1). Twelve hours after 1000 mg/kg MEHP exposure, Tbs1 testicular mRNA levels were induced 114-fold. For most genes, the direction of expression change was constant for all dose levels. However, a related set of genes involved in cholesterol metabolism or steroidogenesis showed a unique, dose-dependent expression pattern. At 1000 mg/kg MEHP, *Cyp17a1*, *StAR*, and *Dhcr7* were decreased 6 h following exposure, but lower MEHP dose levels produced an increased expression of these genes by 12 h (Fig. 3). A similar pattern was observed for *Nr0b1*.

Comparison of the Fetal- and Prepubertal Phthalate–Exposed Testis Gene Profile

As described in the "Introduction" section, the rat testis is susceptible to injury at both the fetal and postnatal time periods, although the morphological outcomes are disparate. To determine the similarity in genetic response within hours of phthalate exposure between these two ages, a comparison was performed between the prepubertal MEHP gene profile and a DBP-exposure study previously performed on the fetal rat testis (Thompson *et al.*, 2005). *In vivo*, DEHP is metabolized quantitatively to its proximal toxicant MEHP, and the effects of DBP and DEHP on fetal testicular gene expression are similar (Liu *et al.*, 2005). For the fetal and prepubertal phthalate exposure comparison, the primary Affymetrix probe level data from the fetal 500 mg/kg DBP exposure were subjected to the same statistical analysis as performed for the prepubertal 1000 mg/kg MEHP exposure. With this analysis applied, approximately 500 unique genes were altered significantly at 1, 3, 6, or 18 h following fetal DBP exposure (Supplementary Table 2).

Merging the prepubertal and fetal microarray datasets using either gene symbol or Unigene identifiers produced a subset of genes with modified expression at both ages. Out of the 500 fetal and 1675 prepubertal genes, 176 showed altered expression at both ages (Fig. 4 and Supplementary Table 3). By categorizing the percentage of identical genes at various time points after exposure, the data revealed that genes with changed expression within 3 h of exposure were more likely to be altered in the other age group. For example, nearly 60% of the genes modified up to 3 h of prepubertal MEHP exposure also were modified within the DBP-exposed fetal testis. Genes encoding

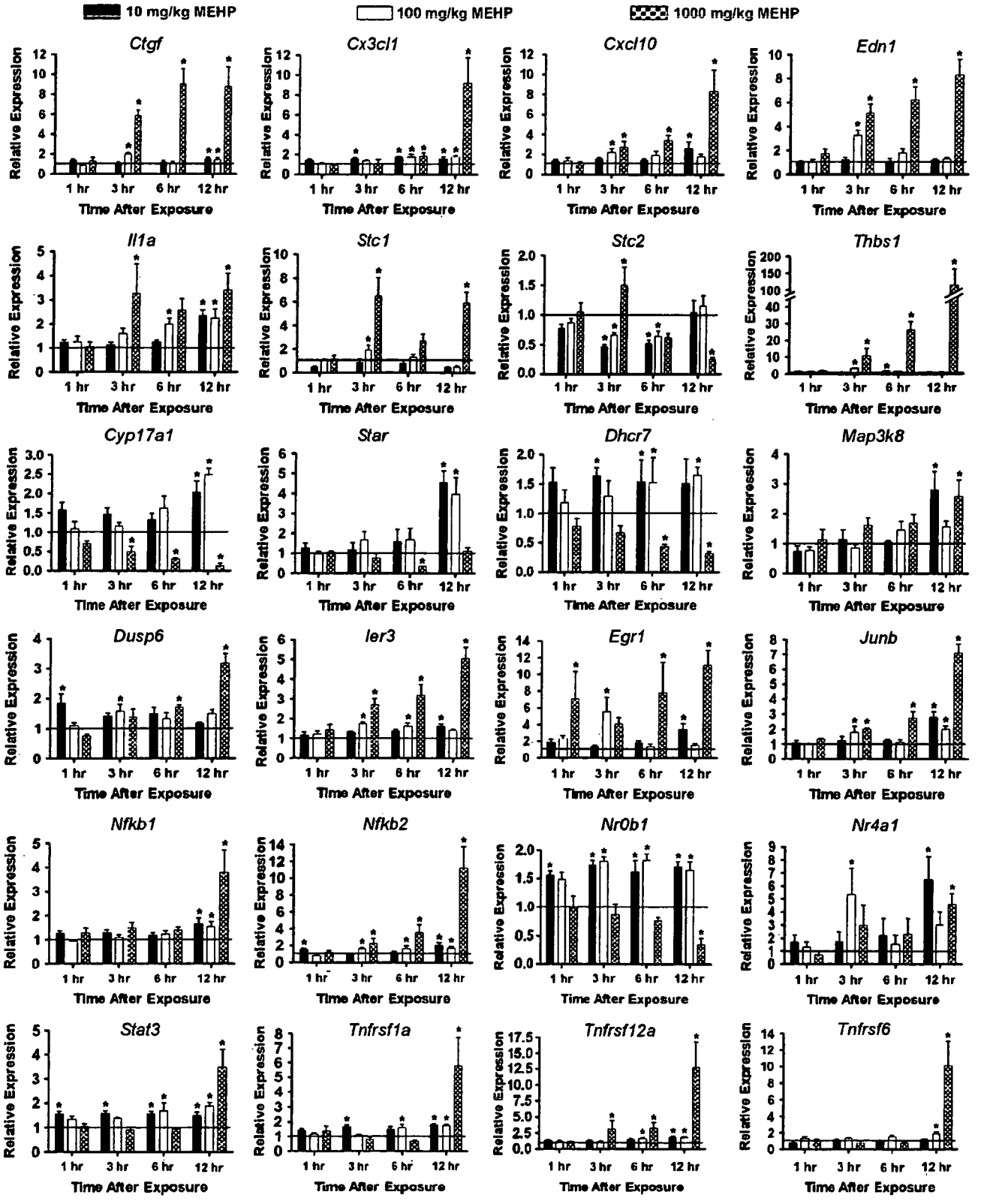
10 mg/kg MEHP
100 mg/kg MEHP
1000 mg/kg MEHP
Ctgf
Cx3cl1
Cxcl10
Edn1
Il1a
Stc1
Stc2
Thbs1
Cyp17a1
Star
Dhcr7
Map3k8
Dusp6
Ier3
Egr1
Junb
Nfkb1
Nfkb2
Nr0b1
Nr4a1
Stat3
Tnfrsf1a
Tnfrsf12a
Tnfrsf6
Relative Expression
Time After Exposure
1 hr
3 hr
6 hr
12 hr

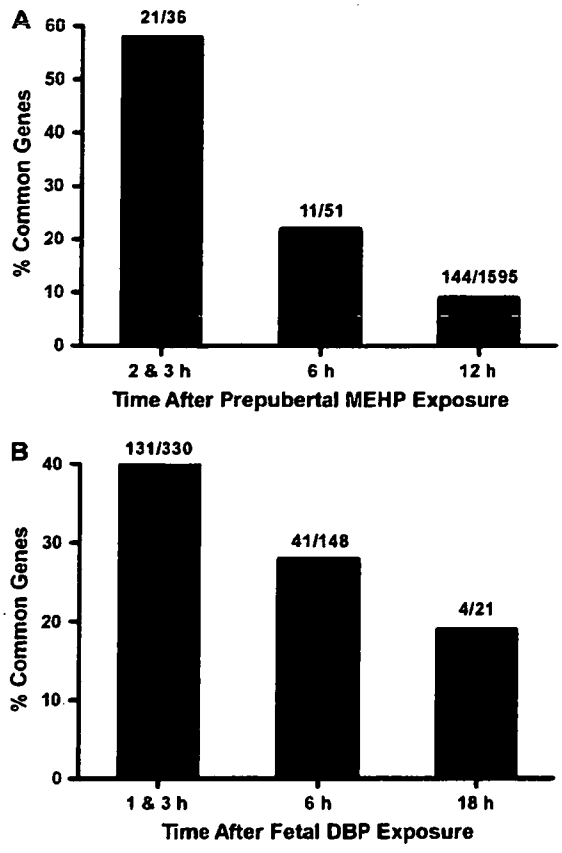

FIG. 4. Percentage of testicular genes with altered expression that were identified following both fetal and prepubertal phthalate exposure. (A) Novel genes with altered expression at each time point after prepubertal MEHP exposure were compared to genes with altered expression at any time point following fetal DBP exposure. For each prepubertal exposure time point, this ratio was determined. Ratios are shown above each bar. (B) The graph shows the reciprocal comparison to that shown in (A). Here, novel genes at each time point after fetal DBP exposure were compared to all prepubertal MEHP time points. In total, there were 176 common genes identified between prepubertal and fetal phthalate exposures.

transcription, intracellular signaling, and secreted factors were prominent functional categories of the common genes (shaded genes in Tables 3 and 4). For nearly all common genes, the direction of change was the same for fetal and prepubertal exposure. At later exposure times (6, 12, and 18 h), the percentage of common genes was reduced. Notably, genes potentially involved in germ cell apoptosis following prepubertal MEHP exposure did not show significant expression changes in the DBP-exposed fetal testis.

DISCUSSION

Despite decades of scrutiny, the phthalate molecular mechanism and testicular target cell leading to adverse effects on testicular function remain unknown (Boekelheide, 2004). Based upon molecular end points and histopathology (Creasy *et al.*, 1983; Rasoulpour and Boekelheide, 2005; Richburg and Boekelheide, 1996; Thompson *et al.*, 2005), the fetal and prepubertal rat testes clearly respond within hours to high-dose phthalate exposure. The genome-wide transcriptional profiling reported here aimed to reveal the initial genetic response of the phthalate-exposed prepubertal testis and use these data in two ways: (1) to develop testable hypotheses on the molecular mechanism of phthalate testicular toxicity and (2) to compare the molecular response of the prepubertal rat testis with that of the fetal rat testis.

The genes first responding to prepubertal phthalate exposure implied that at least two signal transduction pathways were activated immediately. Because our analysis was based upon a whole testis sample, it was not clear which testicular cell types were responsible for changes in gene expression. Within 3 h of exposure, a number of genes with increased expression fell within the class of immediate early response genes that are induced by numerous stimuli. Immediate activation of NF-κB signaling was implied by increased expression of NF-κB negative-feedback loop components known to be induced in response to NF-κB activation; three such components were *Nfkbia* (coding for Ikbα; inhibitory kappaB alpha), *Nfkbiz*, and *Tnfaip3* (which produces the protein A20) (Heyninck and Beyaert, 2005). These results corroborate previous reports of testicular NF-κB activation within 1 h of high-dose phthalate exposure (Rasoulpour and Boekelheide, 2005). Three mRNAs in the sprouty family of receptor tyrosine kinase pathway inhibitors (Spry1, 2, and 4) were induced, which suggests phthalate-induced activation of a mitogen-activated protein kinase (MAPK) pathways (Mason *et al.*, 2006). Additional support for MAPK pathway modulation comes from overexpression of three MAPK phosphatases (Dusp1, 5, and 6).

One potential avenue phthalate exposure may use to induce these signaling pathways is activation of G protein–coupled receptor (GPCR) signaling. It is now clear that downstream

FIG. 3. Phthalate dose- and time-dependence of prepubertal testis gene expression. Gene expression levels relative to an internal calibrator were determined using Taqman-based qPCR. Values for phthalate exposure time points represent the average ± mean. Control values are shown by the horizontal line. *Ctgf* (connective tissue growth factor); *Cx3cl1* [chemokine (C-X3-C motif) ligand 1]; *Cxcl10* [chemokine (C-X-C motif) ligand 10]; *Edn1* (endothelin 1); *Il1a* (interleukin 1 alpha); *Stc1* (stanniocalcin 1); *Stc2* (stanniocalcin 2); *Thbs1* (thrombospondin 1); *Cyp17a1* (cytochrome P450, family 17, subfamily A, polypeptide 1); *StAR* (steroidogenic acute regulatory protein); *Dhcr7* (7-dehydrocholesterol reductase); *Map3k8* (mitogen activated protein kinase kinase kinase 8); *Dusp6* (dual specificity phosphatase 6); *Ier3* (immediate early response 3); *Egr1* (early growth response 1); *Junb* (Jun-B oncogene); *Nfkb1* (nuclear factor of kappa light polypeptide gene enhancer in B-cells 1); *Nfkb2* (nuclear factor of kappa light polypeptide gene enhancer in B-cells 2); *Nr0b1* (nuclear receptor subfamily 0, group B, member 1); *Nr4a1* (nuclear receptor subfamily 4, group A, member 1); *Stat3* (signal transducer and activator of transcription 3); *Tnfrsf1a* (TNFR superfamily, member 1a); *Tnfrsf12a* (TNFR superfamily, member 12A); and *Tnfrsf6* (TNFR superfamily, member 6). $^*p < 0.05$.

TABLE 4
Functional Categorization of Genes Significantly Altered at 6 h after Prepubertal 1000 mg/kg MEHP Exposure[a]

Gene	Affymetrix ID	Functional category
Jub	1373122_at	Signal transducer activity
Mtus1	1380321_at	Signal transducer activity
Nfkbiz_predicted	1378032_at	Signal transducer activity
Pld1	1370530_a_at	Signal transducer activity
Rin3	1375020_at	Signal transducer activity
Rnd1	1381533_at	Signal transducer activity
Sh3md2	1397620_at	Signal transducer activity
Cdk5r1_similar	1377975_at	Signal transducer activity
Txk	1386162_at	Signal transducer activity
Atf3	1369268_at	Transcription regulator activity
Bcl6	1379368_at	Transcription regulator activity
Egr3	1392791_at	Transcription regulator activity
Egr4	1387442_at	Transcription regulator activity
Fos	1375043_at	Transcription regulator activity
Maff	1380229_at	Transcription regulator activity
Mafk	1372211_at	Transcription regulator activity
Mycn	1376648_at	Transcription regulator activity
Nfkb2	1375989_a_at	Transcription regulator activity
Zfp36	1387870_at	Transcription regulator activity
Cdo1	1367755_at	Metabolism
Dhcr7	1368189_at	Metabolism
Fmo2	1377635_at	Metabolism
Fmo3	1368304_at	Metabolism
LOC361349	1390790_a_at	Metabolism
Them2	1388497_at	Metabolism
Ccrl2	1398591_at	Integral to membrane
Cd69	1384837_at	Integral to membrane
Kcnk6	1387264_at	Integral to membrane
Prl	1388103_at	Integral to membrane
Ctsl	1370245_at	Extracellular region
Efnb2_homolog	1383353_at	Extracellular region
Thbs1	1374529_at	Extracellular region
Map1b	1395172_at	Cytoskeletal
Stxbp6	1372681_at	Membrane transport
—	1372490_at	Unknown
—	1372539_at	Unknown
—	1378090_at	Unknown
—	1378561_at	Unknown
—	1378593_at	Unknown
—	1378754_at	Unknown
—	1378778_a_at	Unknown
—	1382031_at	Unknown
—	1392971_at	Unknown
—	1393303_at	Unknown
—	1397577_at	Unknown
LOC314860	1397897_x_at	Unknown
LOC315163	1383490_at	Unknown
LOC499856	1393696_at	Unknown
MGC94198	1397579_x_at	Unknown
Susd3	1379960_at	Unknown
Zc3h12a	1393140_at	Unknown

[a]Genes shaded in gray showed significant expression changes via microarray analysis in the fetal rat testis within 18 h of 500 mg/kg DBP exposure.

GPCR signaling involves stimulation of both MAPK and NF-κB (Gao *et al.*, 2004; Luttrell and Lefkowitz, 2002). Three pieces of evidence suggest that phthalate exposure induces a rapid, GPCR-based response. First, altered expression of a variety of GPCR-related genes was observed in the prepubertal testis exposed to MEHP, among them *Adcy9*, *Gnai1*, *Gpsm1*, *Gprk5* and, conspicuously, a family of sphingosine-1-phosphate GPCRs (*Edg1*, *2*, *3*, and *5*). The potential involvement of Edg receptors in fetal testis phthalate exposure was noted previously (Thompson *et al.*, 2005). Second, phthalate exposure of primary Sertoli cells was shown to modulate the signaling activity of the follicle stimulating hormone receptor (a GPCR) (Lloyd and Foster, 1988). Lastly, phthalate exposure modified the phosphorylation status of a transfected GPCR in Hela cells within minutes (Lahousse *et al.*, 2006). Despite these intriguing results, the molecular basis for activation of signaling pathways in response to phthalate exposure remains an enigma.

The apparent cellular stress in the testis caused by phthalate exposure leads to an increase in germ cell apoptosis. Dose-response data showed an increase in germ cell apoptosis at all MEHP levels examined. The prepubertal gene profiling data presented here suggested that the TNFR family–mediated extrinsic apoptotic pathway was activated. Fas receptor signaling activity is known to mediate some of the phthalate-induced germ cell apoptosis (Richburg *et al.*, 2000), and our results support the role for increased expression of the Fas receptor. However, our gene profiling data suggest the involvement of other pathways. A number of genes associated with the canonical tumor necrosis factor (TNF) alpha apoptotic signaling pathway were induced (Fig. 5A). There was a trend toward increasing expression of the gene encoding TNF alpha at 3 h, prior to an increase in TUNEL-positive germ cells. Most other components of the canonical TNF apoptotic pathway, including TNFR family members and effector proteins, were not induced until 12 h. Similar to another report (Kijima *et al.*, 2004), gene profiling suggested that caspase 3 was a major effector caspase executing phthalate-induced germ cell apoptosis.

Caspase activation leading to cell death also may proceed via a mitochondrial (intrinsic) pathway downstream of JNK activation. Prepubertal phthalate gene profiling also implied that the JNK apoptotic pathway was induced. JNK is activated by phosphorylation mediated via assembly of a protein complex containing scaffolding proteins, mixed lineage kinases, and MAP kinase kinase (MKK) 4 or 7 (both JNK kinases) (Kukekov *et al.*, 2006). After prepubertal MEHP exposure, induction of genes encoding both MKK4 (*Map2k4*) and the JNK scaffolding protein POSH (Plenty Of SH3 Domains; *Sh3md2*) was suggested as early as 2 h. Because overexpression of either MKK4 or POSH can lead to apoptosis (Kukekov *et al.*, 2006), the early increase in MKK4 and POSH mRNA levels suggested that these proteins may be directly involved in phthalate-induced germ cell apoptosis.

A second group of proteins that may be involved in the mitochondrial pathway of germ cell apoptosis is the secreted

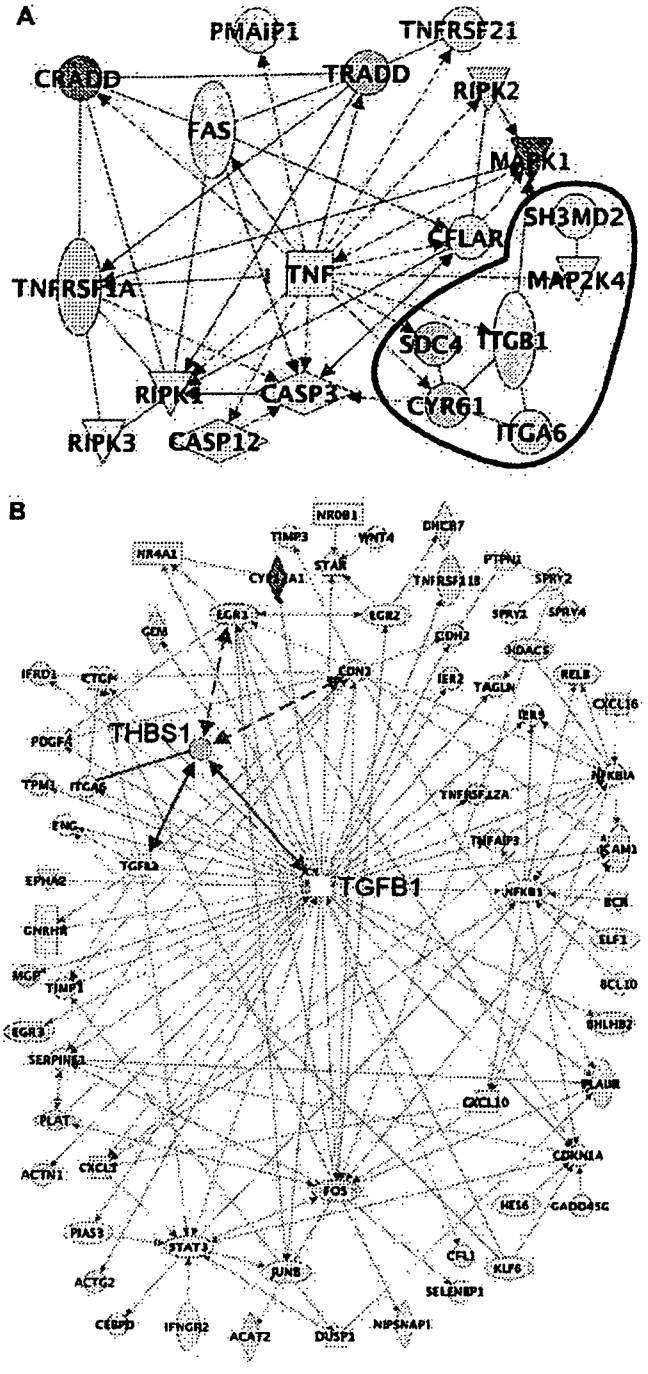

FIG. 5. Network analysis of testicular genes with altered expression following phthalate exposure. The intensity of each node (gene) represents the degree of increased (yellow) or decreased (blue) expression. Lines between nodes represent either scientific literature-based direct (solid) or indirect (dashed) interactions. (A) This network depicts a subset of genes identified in the prepubertal testis MEHP exposure microarray experiment that were known to be involved in apoptosis regulation/induction. Genes within the line in the bottom right corner have been shown to induce the mitochondrial (intrinsic) apoptotic pathway, while the other genes regulate the TNFR-based extrinsic apoptotic pathway. (B) Genes common to both fetal and prepubertal phthalate exposure were used to generate this network. Tbs1 interactions are highlighted in purple. Because *Tgfb1* expression was not changed significantly in the prepubertal microarray experiment, its node is not colored.

protein Cyr61 and its receptors syndecan-4 (Sdc4) and integrin alpha6beta 1 (a6b1). A recent report has causally linked the induction of the fibroblast mitochondrial apoptosis pathway and subsequent activation of caspase 3 to interaction of Cyr61 with both Sdc4 and a6b1 (Todorovicc *et al.*, 2005). Like expressions of POSH and MKK4, testicular mRNA levels for Sdc4, Itga6 (integrin alpha6), and Cyr61 appeared induced hours prior to germ cell DNA fragmentation. Numerous genes potentially involved in prepubertal phthalate–induced germ cell apoptosis (*Tnf*, *Tnfrsf1a*, *Tnfrsf6*, *Tnfrsf21*, *Ripk1*, *Tradd*, *Cradd*, *Casp3*, *Map2k4*, *Sh3md2*, *Cyr61*, and *Sdc4*) were not altered significantly following fetal rat phthalate exposure. Because high-dose fetal exposure does not lead to increased apoptosis (Kleymenova *et al.*, 2005), this result lends additional support to their involvement in prepubertal apoptotic induction.

For some prepubertal testis end points, phthalate exposure produces an interesting response at different dose levels or time points. In the data described here, expression of genes involved in cholesterol metabolism (*Dhcr7*), steroidogenesis (*Cyp17a1* and *StAR*), and one other (*Nr0b1*) was decreased at 1000 mg/kg MEHP but increased at lower MEHP dose levels. The increase in steroidogenic gene expression at 10 and 100 mg/kg MEHP is corroborated by results showing increased testicular testosterone levels in rats following PND21 to 48 phthalate exposure at comparable dose levels (Akingbemi *et al.*, 2001). A similar biphasic response, but over time and not dose, is observed for phthalate-induced germ cell apoptosis; prior to an induction in apoptosis, a decrease often is apparent (Rasoulpour and Boekelheide, 2005). With the available data, it is unclear if the same molecular pathway is being stimulated at a lower phthalate dose level and repressed at a higher dose level or if the high-dose level perturbs an additional pathway.

Although fetal and prepubertal testes contain cell types at divergent states of differentiation, a strikingly high degree of conservation was observed among genes altered following fetal and prepubertal phthalate exposure. The similar genetic response was evident especially at the early time points of exposure during which approximately 50% of the reactive genes were the same. Over time, the fetal and prepubertal testis gene profiles diverged, and this may reflect the differing histopathology observed; the prepubertal testis initiated germ cell apoptosis and showed a neutrophil infiltrate while these changes were not observed in DBP-exposed fetal rat testis (Kleymenova *et al.*, 2005). Furthermore, the methodologies used in the fetal and prepubertal microarray analyses varied in three ways: (1) use of different phthalate congeners (DBP vs. MEHP); (2) dose levels (500 mg/kg DBP vs. 1000 mg/kg MEHP); and (3) time-point selection. While all time points of

prepubertal exposure were examined on a single genome-wide Affymetrix chip, the fetal experiments were performed with two separate Affymetrix chips (RAE230 A and B) and only the 1- and 3-h time points were analyzed on both chips. Given these differences, it is likely that the degree of similarity in genetic response between the phthalate-exposed fetal and prepubertal testis described here is a conservative estimation. Overall, these data following fetal and prepubertal phthalate exposure suggest a common initial molecular and cellular testicular response followed by divergent histopathology due to differences in cellular differentiation state and/or tissue architecture.

To gain insight into the phthalate toxicity mechanism, network analysis of the genes with altered expression following both fetal and prepubertal exposure was performed (Fig. 5B). Because interaction linkages could not be detected for all genes using Ingenuity software, only a subset of genes was included in the network analysis. In the prepubertal testis, a large increase in Tbs1 mRNA levels was noted which began 2 h following 1000 mg/kg MEHP exposure, and by 3 and 12 h, Tbs1 mRNA levels were induced 10- and 114-fold, respectively. A similar increase occurs between 1 and 3 h in the fetal testis following 500 mg/kg DPB exposure (Thompson *et al.*, 2005). This robust and early increase suggested a potentially critical role in downstream adverse testicular outcomes. Tbs1 is a secreted matricellular protein with numerous functional activities, including tissue remodeling and modulation of growth factor/cytokine responses (Chen *et al.*, 2000). Although it binds to several different transmembrane receptors and cell surface proteins, integrins are one of the major Tbs1 receptors. Among Tbs1 integrin receptors, Itga6 expression appeared increased in the testis 3 h after fetal and prepubertal phthalate exposure. Another matricellular integrin ligand (connective tissue growth factor; Ctgf) was induced within hours of fetal and prepubertal phthalate exposure (Heng *et al.*, 2006). Based upon increased expression of integrins and integrin ligands as well as the seminal role of integrins in tissue morphogenesis (De Arcangelis and Georges-Labouesse, 2000), an attractive hypothesis for some of the abnormal fetal testis morphogenesis observed following phthalate exposure is that it results from aberrant integrin-based cell adhesion and/or migration (Mahood *et al.*, 2005).

In addition to a cell adhesion/migration function, Tbs1 can influence growth factor function. *In vivo*, Tbs1 activates the latent form of transforming growth factor beta 1 (Tgfb1), inducing Tgfb1 signaling events (Crawford *et al.*, 1998). When Tgfb1 was included in the network analysis of common fetal and prepubertal genes, interaction of a large majority of the phthalate-altered genes with Tgfb1 was obvious (Fig. 5B). This network analysis supports the hypothesis that Tbs1 induction after phthalate exposure may produce an increase in active Tgfb1. A phthalate-induced decrease in testicular steroidogenic gene expression and testosterone production is a prominent outcome of exposure (Lehmann *et al.*, 2004), and active Tgfb1 has been shown to decrease steroidogenic enzyme gene expression (Brand *et al.*, 2000) and Leydig cell steroidogenesis (Gnessi *et al.*, 1997). Thus, although Tgfb1 mRNA levels were not changed following phthalate exposure in the microarray analysis, we speculate that phthalate-induced decreases in testicular steroidogenesis may result from induction of Tbs1 protein secretion followed by Tbs1 activation of extracellular latent Tgfb1.

In conclusion, the data reported here showed that a single prepubertal exposure to 1000 mg/kg MEHP resulted in altered expression of many testicular genes related to intracellular signaling, cellular interactions, and gene transcription. At a MEHP dose level of 10 mg/kg, induction of germ cell apoptosis occurred, and nearly all genes tested by qPCR were changed significantly. Finally, the prepubertal testis genetic response appeared similar to that of the fetal testis following DBP exposure. These data suggest a common initial molecular mechanism of phthalate testicular toxicity following both prepubertal and fetal exposure.

SUPPLEMENTARY DATA

Supplementary data are available online at http://toxsci.oxfordjournals.org/.

ACKNOWLEDGMENTS

The authors wish to thank Linda Pluta for performing the microarray procedures and Drs. Rusty Thomas and Dave Dorman for reviewing the manuscript. This research was funded through the Long Range Research Initiative of the American Chemistry Council.

REFERENCES

Akingbemi, B. T., Youker, R. T., Sottas, C. M., Ge, R., Katz, E., Klinefelter, G. R., Zirkin, B. R., and Hardy, M. P. (2001). Modulation of rat Leydig cell steroidogenic function by di(2-ethylhexyl) phthalate. *Biol. Reprod.* **65**, 1252–1259.

Boekelheide, K. (2004). Cracking the nut. *Toxicol. Sci.* **81**, 1–2.

Boekelheide, K., Johnson, K. J., and Richburg, J. H. (2004). Sertoli cell toxicants. In *Sertoli Cell Biology* (M. K. Skinner and M. D. Griswold, Eds.), pp. 345–382. Academic Press, San Diego, CA.

Brand, C., Nury, D., Chambaz, E. M., Feige, J. J., and Bailly, S. (2000). Transcriptional regulation of the gene encoding the StAR protein in the human adrenocortical cell line, H295R by cAMP and TGFbeta1. *Endocr. Res.* **26**, 1045–1053.

Cai, L., Chen, S., Evans, T., Deng, D. X., Mukherjee, K., and Chakrabarti, S. (2000). Apoptotic germ-cell death and testicular damage in experimental diabetes: Prevention by endothelin antagonism. *Urol. Res.* **28**, 342–347.

Chen, H., Herndon, M. E., and Lawler, J. (2000). The cell biology of thrombospondin-1. *Matrix Biol.* **19**, 597–614.

Chu, T. M., Weir, B., and Wolfinger, R. (2002). A systematic statistical linear modeling approach to oligonucleotide array experiments. *Math. Biosci.* **176**, 35–51.

Crawford, S. E., Stellmach, V., Murphy-Ullrich, J. E., Ribeiro, S. M., Lawler, J., Hynes, R. O., Boivin, G. P., and Bouck, N. (1998). Thrombospondin-1 is a major activator of TGF-beta1 in vivo. *Cell* **93**, 1159–1170.

Creasy, D. M., Foster, J. R., and Foster, P. M. (1983). The morphological development of di-N-pentyl phthalate induced testicular atrophy in the rat. *J. Pathol.* **139,** 309–321.

De Arcangelis, A., and Georges-Labouesse, E. (2000). Integrin and ECM functions: Roles in vertebrate development. *Trends Genet.* **16,** 389–395.

Friedl, P., Vischer, P., and Freyberg, M. A. (2002). The role of thrombospondin-1 in apoptosis. *Cell. Mol. Life Sci.* **59,** 1347–1357.

Gao, H., Sun, Y., Wu, Y., Luan, B., Wang, Y., Qu, B., and Pei, G. (2004). Identification of beta-arrestin2 as a G protein-coupled receptor-stimulated regulator of NF-kappaB pathways. *Mol. Cell* **14,** 303–317.

Gentleman, R. C., Carey, V. J., Bates, D. M., Bolstad, B., Dettling, M., Dudoit, S., Ellis, B., Gautier, L., Ge, Y., Gentry, J., *et al.* (2004). Bioconductor: Open software development for computational biology and bioinformatics. *Genome Biol.* **5,** R80.

Gnessi, L., Fabbri, A., and Spera, G. (1997). Gonadal peptides as mediators of development and functional control of the testis: An integrated system with hormones and local environment. *Endocr. Rev.* **18,** 541–609.

Hales, D. B. (2002). Testicular macrophage modulation of Leydig cell steroidogenesis. *J. Reprod. Immunol.* **57,** 3–18.

Heng, E. C., Huang, Y., Black, S. A. Jr, and Trackman, P. C. (2006). CCN2, connective tissue growth factor, stimulates collagen deposition by gingival fibroblasts via module 3 and alpha6- and beta1 integrins. *J. Cell. Biochem.* **98,** 409–420.

Hess, J., Angel, P., and Schorpp-Kistner, M. (2004). AP-1 subunits: Quarrel and harmony among siblings. *J. Cell Sci.* **117,** 5965–5973.

Heyninck, K., and Beyaert, R. (2005). A20 inhibits NF-kappaB activation by dual ubiquitin-editing functions. *Trends Biochem. Sci.* **30,** 1–4.

Jo, Y., and Stocco, D. M. (2004). Regulation of steroidogenesis and steroidogenic acute regulatory protein in R2C cells by DAX-1 (dosage-sensitive sex reversal, adrenal hypoplasia congenita, critical region on the X chromosome, gene-1). *Endocrinology* **145,** 5629–5637.

Jordan, B. K., Shen, J. H., Olaso, R., Ingraham, H. A., and Vilain, E. (2003). Wnt4 overexpression disrupts normal testicular vasculature and inhibits testosterone synthesis by repressing steroidogenic factor 1/beta-catenin synergy. *Proc. Natl. Acad. Sci. U.S.A.* **100,** 10866–10871.

Kijima, K., Toyosawa, K., Yasuba, M., Matsuoka, N., Adachi, T., Komiyama, M., and Mori, C. (2004). Gene expression analysis of the rat testis after treatment with di(2-ethylhexyl) phthalate using cDNA microarray and real-time RT-PCR. *Toxicol. Appl. Pharmacol.* **200,** 103–110.

Kim, J., Lee, Y. H., Kwon, T. K., Chang, J. S., Chung, K. C., and Min do, S. (2006). Phospholipase D prevents etoposide-induced apoptosis by inhibiting the expression of early growth response-1 and phosphatase and tensin homologue deleted on chromosome 10. *Cancer Res.* **66,** 784–793.

Kleymenova, E., Swanson, C., Boekelheide, K., and Gaido, K. W. (2005). Exposure in utero to di(n-butyl) phthalate alters the vimentin cytoskeleton of fetal rat Sertoli cells and disrupts Sertoli cell-gonocyte contact. *Biol. Reprod.* **73,** 482–490.

Kruse, M. L., Arlt, A., Sieke, A., Grohmann, F., Grossmann, M., Minkenberg, J., Folsch, U. R., and Schafer, H. (2005). Immediate early gene X1 (IEX-1) is organized in subnuclear structures and partially co-localizes with promyelocytic leukemia protein in HeLa cells. *J. Biol. Chem.* **280,** 24849–24856.

Kukekov, N. V., Xu, Z., and Greene, L. A. (2006). Direct interaction of the molecular scaffolds POSH and JIP is required for apoptotic activation of JNKs. *J. Biol. Chem* **281,** 15517–15524.

Lahousse, S. A., Beall, S. A., and Johnson, K. J. (2006). Mono-(2-ethylhexyl) phthalate rapidly increases celsr2 protein phosphorylation in HeLa cells via protein kinase C and casein kinase 1. *Toxicol. Sci.* **91,** 255–264.

Lau, L. F., and Lam, S. C. T. (2005). Integrin-mediated CCN functions. In *CCN Proteins: A New Family of Cell Growth and Differentiation Regulators* (B. Perbal and M. Takigawa, Eds.), pp. 61–79. Imperial College Press, London.

Lehmann, K. P., Phillips, S., Sar, M., Foster, P. M., and Gaido, K. W. (2004). Dose-dependent alterations in gene expression and testosterone synthesis in the fetal testes of male rats exposed to di(n-butyl) phthalate. *Toxicol. Sci.* **81,** 60–68.

Liu, K., Lehmann, K. P., Sar, M., Young, S. S., and Gaido, K. W. (2005). Gene expression profiling following in utero exposure to phthalate esters reveals new gene targets in the etiology of testicular dysgenesis. *Biol. Reprod.* **73,** 180–192.

Lloyd, S. C., and Foster, P. M. (1988). Effect of mono-(2-ethylhexyl) phthalate on follicle-stimulating hormone responsiveness of cultured rat Sertoli cells. *Toxicol. Appl. Pharmacol.* **95,** 484–489.

Lu, D., Wolfgang, C. D., and Hai, T. (2006). Activating transcription factor 3, a stress-inducible gene, suppresses ras-stimulated tumorigenesis. *J. Biol. Chem.* **281,** 10473–10481.

Lukyanenko, Y. O., Chen, J. J., and Hutson, J. C. (2001). Production of 25-hydroxycholesterol by testicular macrophages and its effects on Leydig cells. *Biol. Reprod.* **64,** 790–796.

Luttrell, L. M., and Lefkowitz, R. J. (2002). The role of beta-arrestins in the termination and transduction of G-protein-coupled receptor signals. *J. Cell Sci.* **115,** 455–465.

Mahood, I. K., Hallmark, N., McKinnell, C., Walker, M., Fisher, J. S., and Sharpe, R. M. (2005). Abnormal Leydig cell aggregation in the fetal testis of rats exposed to di(n-butyl) phthalate and its possible role in testicular dysgenesis. *Endocrinology* **146,** 613–623.

Mason, J. M., Morrison, D. J., Basson, M. A., and Licht, J. D. (2006). Sprouty proteins: Multifaceted negative-feedback regulators of receptor tyrosine kinase signaling. *Trends Cell Biol.* **16,** 45–54.

Moussad, E. E., and Brigstock, D. R. (2000). Connective tissue growth factor: What's in a name? *Mol. Genet. Metab.* **71,** 276–292.

Papa, S., Zazzeroni, F., Bubici, C., Jayawardena, S., Alvarez, K., Matsuda, S., Nguyen, D. U., Pham, C. G., Nelsbach, A. H., Melis, T., *et al.* (2004). Gadd45 beta mediates the NF-kappa B suppression of JNK signalling by targeting MKK7/JNKK2. *Nat. Cell Biol.* **6,** 146–153.

Pfaffl, M. W. (2001). A new mathematical model for relative quantification in real-time RT-PCR. *Nucleic Acids Res.* **29,** e45.

Rasoulpour, R. J., and Boekelheide, K. (2005). NF-kappaB is activated in the rat testis following exposure to mono-(2-ethylhexyl) phthalate. *Biol. Reprod.* **72,** 479–486.

Richburg, J. H., and Boekelheide, K. (1996). Mono-(2-ethylhexyl) phthalate rapidly alters both Sertoli cell vimentin filaments and germ cell apoptosis in young rat testes. *Toxicol. Appl. Pharmacol.* **137,** 42–50.

Richburg, J. H., and Nanez, A. (2003). Fas- or FasL-deficient mice display an increased sensitivity to nitrobenzene-induced testicular germ cell apoptosis. *Toxicol. Lett.* **139,** 1–10.

Richburg, J. H., Nanez, A., Williams, L. R., Embree, M. E., and Boekelheide, K. (2000). Sensitivity of testicular germ cells to toxicant-induced apoptosis in gld mice that express a nonfunctional form of Fas ligand. *Endocrinology* **141,** 787–793.

Silva, M. J., Barr, D. B., Reidy, J. A., Malek, N. A., Hodge, C. C., Caudill, S. P., Brock, J. W., Needham, L. L., and Calafat, A. M. (2004). Urinary levels of seven phthalate metabolites in the U.S. population from the National Health and Nutrition Examination Survey (NHANES) 1999-2000. *Environ. Health Perspect.* **112,** 331–338.

Thompson, C. J., Ross, S. M., Hensley, J., Liu, K., Heinze, S. C., Young, S. S., and Gaido, K. W. (2005). Differential steroidogenic gene expression in the fetal adrenal gland versus the testis and rapid and dynamic response of the fetal testis to di(n-butyl) phthalate. *Biol. Reprod.* **73,** 908–917.

Todorovicc, V., Chen, C. C., Hay, N., and Lau, L. F. (2005). The matrix protein CCN1 (CYR61) induces apoptosis in fibroblasts. *J. Cell Biol.* **171,** 559–568.

Xi, H., and Kersh, G. J. (2004). Sustained early growth response gene 3 expression inhibits the survival of CD4/CD8 double-positive thymocytes. *J. Immunol.* **173,** 340–348.

Toxicology, 34 (1985) 13—27
Elsevier Scientific Publishers Ireland Ltd.

EFFECT OF PHTHALATE ESTERS ON ENERGY COUPLING AND SUCCINATE OXIDATION IN RAT LIVER MITOCHONDRIA

RONALD L. MELNICK[a] and CAROL M. SCHILLER[b]

[a]*National Toxicology Program and* [b]*Laboratory of Pharmacology, National Institute of Environmental Health Sciences, Research Triangle Park, NC 27709 (U.S.A.)*

(Received July 5th, 1984)
(Accepted September 21st, 1984)

SUMMARY

Isolated rat liver mitochondira were exposed to mono- and di-*n*-butyl phthalate (MBP and DBP) and mono- and di(2-ethylhexyl)phthalate (MEHP and DEHP) and examined for effects on mitochondrial energy-dependent processes, including oxidative phosphorylation and active K^+ uptake. Additional studies on the effects of these phthalate esters on succinate oxidation and on mitochondrial membrane integrity are also included. DBP and MEHP stimulated succinate state 4 respiration, impaired K^+-valinomycin induced swelling with succinate, ascorbate, or ATP as the energy sources, and inhibited succinate state 3 respiration and succinate cytochrome *c* reductase activity. MEHP was found to act as a non-competitive inhibitor of succinate dehydrogenase activity, with an apparent $K_i = 2.4 \times 10^{-4}$ M. At concentrations which uncouple energy linked reactions, MEHP and DBP produced only slight energy-independent swelling and release of soluble proteins from isolated mitochondria. MBP caused only slight stimulation of state 4 respiration and impairment of K^+-valinomycin induced swelling with each of the 3 energy sources, however, of the 4 phthalate esters, it produced the greatest energy-independent swelling and led to the greatest release of soluble mitochondrial proteins. DEHP had no apparent effect on any of these processes except for slight impairment of ATP-dependent K^+-valinomycin induced swelling. It is concluded that phthalate ester toxicity in liver

Address all correspondence to: Dr. Ronald L. Melnick, National Institute of Environmental Health Sciences, P.O. Box 12233, Research Triangle Park, NC 27709, U.S.A. (919) 541-4142.

Abbreviations: DEHP, di(2-ethylhexyl)phthalate; MEHP, mono(2-ethylhexyl)phthalate; DBP, di-*n*-butyl phthalate; MBP, mono-*n*-butyl phthalate; SDH, succinate dehydrogenase; TMPD, *N,N,N',N'*-tetramethyl-*p*-phenylenediamine; RCR, respiratory control ratio; FCCP, carbonyl cyanide *p*-trifluoromethoxy phenylhydrazone; OD, optical density, MDH, malate dehydrogenase.

0300-483X/85/$03.30

mitochondria is due to uncoupling of energy linked reactions and/or inhibition of succinate dehydrogenase activity. Uncoupling by MBP may involve disruption of mitochondrial membrane integrity, while uncoupling by DBP and MEHP is probably due to an increase in membrane permeability to H^+ and other small ions.

Key words: Phthalate esters; Mitochondrial uncoupling; Succinate dehydrogenase inhibition

INTRODUCTION

Phthalic acid esters are used extensively as plasticizers in the manufacture of a variety of plastic products, including food packaging materials and polyvinyl chloride (PVC) blood bags. Di(2-ethylhexyl)phthalate (DEHP) and di-*n*-butyl phthalate (DBP) are 2 of the most abundantly produced phthalate ester plasticizers. Since the plasticizer is not chemically bound to the polymeric matrix, leaching of the plasticizer can occur. Phthlate ester plasticizers are found widely distributed in the environment, and DEHP, the most commonly used phthalate ester in PVC products, has been detected at significant levels (0.05 mg/ml of plasma) in human blood stored in PVC bags [1]. These findings have raised concerns of possible toxicological hazards associated with exposure to phthalate ester plasticizers. Phthalate esters, in general, have been considered to possess a low order of toxicity [2]. However, DEHP and other phthalate esters have been shown to produce morphological and functional alterations in liver [3] and to inhibit growth of human cell cultures [4,5]. Concern over DEHP has heightened recently with publication by the National Toxicology Program of a 2-year feeding study in which DEHP was found to be hepatocarcinogenic in rats and mice [6,7].

Mitochondria appear to be a subcellular target structure of phthalate esters. Nazir et al. [8] found DEHP to be specifically localized in heart muscle mitochondria from several species of animals. Lake et al. [3] showed that daily oral administration of DEHP at a dose of 2000 mg/kg for 21 days resulted in swelling of liver mitochondria and depression of succinate dehydrogenase (SDH) activity. Similar biochemical and ultrastructural changes were induced with comparable doses of mono(2-ethylhexyl)phthalate (MEHP) [3], the primary intermediate of DEHP metabolism [9]. Strivastava et al. [10] reported that intraperitoneal injections of DEHP to male rats caused a decrease in liver adenosine triphosphatase (ATPase) and SDH activities. Takahashi [11] showed that the effects of dialkyl and monoalkyl phthalates on respiratory rates of isolated mitochondria varied depending on the length of the alkyl chains. Ohyama [12] and Takahashi [11] concluded that phthalate esters act mainly as electron and energy transfer inhibitors. This conclusion was based largely on the observed inhibitory effects of a variety of phthalate esters on state- 3 respiration rates. Inouye et al. [13] suggested that DBP acts as an uncoupler of oxidative phosphorylation since

it inhibited respiratory control, increased state-4 respiration, stimulated latent mitochondrial ATPase activity, and induced release of K^+ from intact mitochondria.

Alterations in mitochondrial activities may contribute to hepatotoxic effects associated with exposure to phthalate esters. The objectives of the present studies were to characterize the inhibitory effects of phthalate esters on mitochondrial oxidative phosphorylation and other energy-dependent processes, and to further elucidate the mechanism of phthalate ester toxicity in liver mitochondria. DEHP and DBP, and their monoalkyl derivatives (MEHP and MBP) were used in these studies because of their widespread distribution, and because previous studies indicated that they affect mitochondrial respiratory activity [11—13].

MATERIALS AHD METHODS

Chemicals

Reagent grade DBP was obtained from Fisher Scientific Company. Technical grade DEHP was obtained from the Hatco Chemical Division of W.R. Grace and Company. MEHP and MBP were synthesized by refluxing phthalic anhydride and 2-ethylhexanol or *n*-butanol in toluene, and were then extracted as described by Albro et al. [9]. IR spectra, taken as neat films on NaCl plates with a Perkin-Elmer Model 621 spectrophotometer, confirmed the identity of the MEHP and MBP preparations (Albro, pers. commun.). Stock solutions of each of the phthalate esters were made in 95% ethanol.

Preparation of mitochondria

Mitochondria were isolated from the livers of 250 to 300 g male rats of the CD strain, as described by Stancliff et al. [14], in a medium that consisted of 330 mM sucrose, 5 mM Tris—HCl (pH 7.6) and 0.5 mM EGTA.

Assay Methods

Respiratory rates were measured polarographically with a Clark-type oxygen electrode in 2 ml of a medium [15] consisting of 250 mM sucrose, 10 mM KCl, 10 mM Tris—HCl (pH 7.6), 3 mM NaH_2PO_4, 5 mM $MgCl_2$, and 1.8 μg/ml rotenone. Mitochondrial samples (3 mg protein) were incubated at 30°C for 2 min with the phthalate esters prior to the addition of substrate. State 4 respiration was initiated by the addition of succinate (2.0 mM), and phosphorylation (state 3 respiration) was initiated by the addition of 0.25 μmol of ADP. The control samples were incubated with the same final concentration of ethanol (0.24%) that resulted from the addition of the phthalate esters.

Mitochondrial volume changes due to active K^+ uptake were monitored spectrophotometrically at 540 nm. The reaction medium (16) contained 100 mM sucrose, 28.6 mM potassium acetate, 5 mM Tris-acetate (pH 7.6), 1.2 μg/ml rotenone, 0.02 μg/ml valinomycin, and either 2.0 mM succinate, 2.0 mM ascorbate + 0.15 mM TMPD, or 2.0 mM ATP. Mitochondrial samples

(2 mg protein) were added to 3 ml of reaction medium and incubated with the phthalate esters for 2 min prior to the addition of the energy source.

Succinate cytochrome *c* reductase activity was determined [17] by measuring the increase in absorbance at 550 nm in a medium containing 20 mM potassium phosphate (pH 7.5), 2 mM KCN, and 0.15 mM cytochrome *c*. Mitochondrial samples (1 mg) were incubated in 3 ml of the reaction medium to lyse the membranes, and then the phthalate ester was added and the sample was incubated for an additional 2 min. Reduction of cytochrome *c* was initiated by the addition of succinate (2 mM final concentration).

SDH (EC 1.3.991) activity was measured spectrophotometrically [18] at 550 nm at 30°C in 3 ml of a medium containing 50 mM potassium phosphate (pH 7.8), 0.1% BSA, 1 mM EDTA, 2 mM KCN, 0.067 mM cytochrome *c*, 0.017% phenazine methosulfate. Reduction of cytochrome *c* was initiated by the addition of succinate.

Malate dehydrogenase (EC 1.1.1.37) activity was determined by measuring the decrease in absorbance at 340 nm [19] in a medium containing 50 mM Tris–HCl (pH 7.6), 2 mM oxaloacetate, 0.15 mM NADH, and 0.05% Triton X-100.

Protein concentrations were determined by the method of Lowry et al. [20] using bovine serum albumin as a standard.

RESULTS

Effect of phthalate esters on succinate respiration (oxidative phosphorylation)

The effects of MBP, DBP, MEHP and DEHP on succinate respiration rates and respiratory control ratios (RCR) of isolated rat liver mitochondria are shown in Table I. The RCR is a measure of the dependence of the respiratory rate on ADP, and is defined as the rate of respiration in the presence of ADP (state 3) divided by the rate of respiration after complete utilization of ADP (state 4). Except for DEHP, each of the phthalate esters caused stimulation of state 4 respiration. This was most apparent with DBP, and only moderately evident with MBP. In the case of MEHP, stimulation of state 4 respiration was observed at 0.1 mM but not at 1.0 mM concentration.

State 3 respiration rates in the presence of MBP were nearly identical to control state 3 rates. The decrease in respiratory control due to MBP is therefore, attributed to the slight stimulation of state 4 respiration.

State 3 respiration rates were slightly decreased in the presence of 1.0 mM DBP. Such a decrease may be due to inhibition of electron transport activity or of ADP phosphorylation. Due to the near maximal stimulation of succinate respiration by DBP in the absence of ADP (state 4 respiration), the increment in the respiration rate after addition of ADP was very slight. The loss of respiratory control in the presence of DBP is, therefore, attributed largely to stimulation of state 4 respiration, with some contribution at 1.0 mM DBP from inhibition of state 3 respiration.

State 3 respiration rates in the presence of MEHP were lower than the control state 3 rates, and this effect was concentration dependent. At 1.0

TABLE I

EFFECT OF PHTHALATE ESTERS ON MITOCHONDRIAL RESPIRATION[a]

Condition	RCR[b]	natoms oxygen × min^{-1} × mg $protein^{-1}$		
		State 4 rate	State 3 rate	ADP stimulation[c]
Control (0.24% ethanol)	4.0	19.7	78.6	58.9
MBP, 0.1 mM	3.3	23.9	78.4	54.5
MBP, 1.0 mM	3.1	27.9	86.3	58.4
DBP, 0.1 mM	1.3	61.5	80.0	18.1
DBP, 1.0 mM	1.2	56.7	67.1	10.4
MEHP, 0.1 mM	1.7	36.0	62.9	26.9
MEHP, 1.0 mM	—	18.9	16.3	—
DEHP, 0.1 mM	3.9	19.9	78.3	58.4
DEHP, 1.0 mM	3.9	19.9	77.2	57.3

[a]Conditions of the assay are described in Materials and Methods. All measurements were made in duplicate on the same mitochondrial preparation, and the mean values are presented. The results in this table are representative of 3 different preparations.

[b]Respiratory control ratios (RCR = state 3/state 4) were calculated from oxygen uptake traces.

[c]State 3 rate — State 4 rate.

mM MEHP, the state 3 rate was nearly the same as the state 4 rate. The decrease in respiratory control and the low level of ADP stimulation in the presence of 0.1 mM MEHP is due to both stimulation of state 4 respiration and inhibition of state 3 respiration. The apparent lack of stimulation of state 4 respiration at 1.0 mM MEHP, and the decrease in state 3 respiration rates at 0.1 and 1.0 mM concentrations compared to the control rates, are most likely due to inhibition of succinate oxidation. This contention is supported by our finding that respiratory rates were not stimulated by the uncoupler carbonyl cyanide *p*-trifluoromethoxy phenylhydrazone (FCCP) (1.0 μM), but were stimulated maximally by addition of ascorbate plus *N,N,N',N'-tetramethyl-p*-phenylene diamine (TMPD) (results not shown). Since ascorbate + TMPD donate electrons into the electron transport chain at cytochrome *c*, then inhibition of succinate oxidation by MEHP must occur between succinate dehydrogenase and cytochrome *c*.

There was no apparant effect of DEHP on either state 3 or state 4 succinate respiration rates at either concentration.

Effect of phthalate esters on energy-dependent K^+-valinomycin induced swelling

The polarographic studies indicate that some of the phthalate esters may act as uncouplers of oxidative phorphorylation and inhibitors of electron transport activity. To explore these possibilities, we examined the effects of the same phthalate esters on energy-dependent K^+-valinomycin induced swelling. K^+ is naturally impermeable to the inner mitochondrial membrane,

however, the lipid-soluble ionophore, valinomycin, has a polar interior that delocalizes the cationic charge so that the K^+-valinomycin complex can diffuse through the membrane in response to a concentration gradient or an electrical gradient across the inner membrane. The energy-dependent accumulation of K^+ in isolated rat liver mitochondria was monitored spectrophotometrically, and was driven by the oxidation of respiratory chain substrates, succinate or ascorbate + TMPD, or by the hydrolysis of ATP. Changes in OD, due to K^+ uptake and subsequent osmotic water flow which leads to mitochondrial swelling, for selected incubations with the phthalate esters are presented in Fig. 1. In the control suspensions, the maximum amplitude

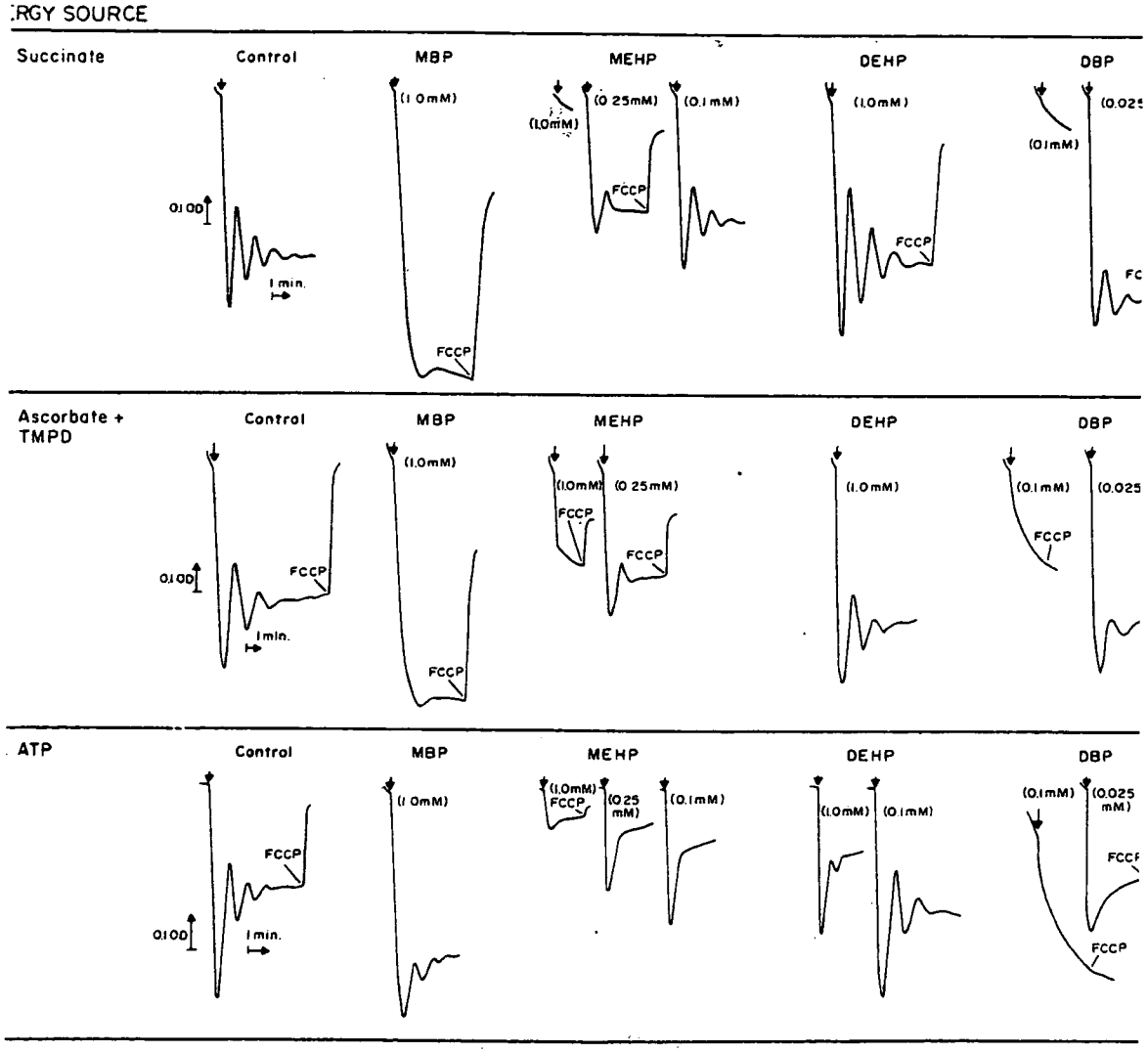

Fig. 1. Effect of MBP, MEHP, DEHP, and DBP on energy-dependent K^+-valinomycin induced swelling of rat liver mitochondria. Phthalate esters dissolved in ethanol were added to the reaction medium and this was followed 2 min later by the addition of either (A) succinate (2.0 mM), (B) ascorbate (2.0 mM) + TMPD (0.15 mM), or (C) ATP (2.0 mM). Arrows indicate when the energy source was added. Mitochondrial volume changes were followed spectrophotometrically at 540 nm. Where indicated, FCCP = 1.0 μM.

of swelling is reached about 30 sec after the addition of the energy source (first tracing of each panel, Fig. 1). The mitochondria then undergo a series of swellings and contractions until the oscillations become damped, largely due to loss in synchrony and to membrane deterioration occurring during the swelling and contraction cycles [16]. The process is sensitive to inhibitors of substrate oxidation, or inhibitors of ATP hydrolysis if ATP is the energy source, or agents that collapse the membrane potential (uncouplers).

Swelling profiles of mitochondrial samples incubated with each of the phthalate esters were obtained with each of the 3 energy sources (Fig. 1). Several representative tracings are presented in Fig. 1, in order to show the concentration dependence of the chemically-induced effects. In the presence of 1.0 mM MBP, swelling was slower but more extensive (greater Δ OD) than for the controls with each of the energy sources, and the oscillations appeared to be damped. The OD changes (swelling) in the presence of 1.0 mM MBP were energy dependent, since they were sensitive to FCCP. Reduction of the concentration of MBP to 0.1 mM resulted in OD changes that were similar to those of the controls (results not shown).

Incubation of mitochondria with 1.0 mM MEHP prevented swelling with succinate as the energy source; however, slight uncoupler sensitive swelling with ascorbate + TMPD or ATP was still observed. This result suggests that MEHP exerts a common effect on mitochondria with each of the 3 energy sources, and an additional effect on succinate oxidation linked swelling. Reduction of the MEHP concentration to 0.25 mM or 0.1 mM partially improved the energy-dependent K^+-valinomycin transport activity in each case.

DEHP at a concentration of 1.0 mM, had no noticeable effect on the swelling traces in which succinate or ascorbate + TMPD served as the energy source. There was a slight impairment in ATP supported K^+ uptake at 1.0 mM DEHP. This effect was specific for ATP hydrolysis and suggests a possible inhibition of Mg^{2+}-ATPase activity or of the adenine nucleotide translocator.

Energy-dependent K^+-valinomycin transport driven by succinate or ascorbate oxidation, or by ATP hydrolysis was prevented completely by 1.0 or 0.1 mM DBP. Some energy linked (FCCP sensitive) swelling was apparent when the concentration of DBP was reduced to 0.025 mM. At 0.01 mM DBP, swelling traces were similar to those of the controls (results not shown).

Inhibition of SDH Activity

The inhibition of succinate state 3 respiration rates by DBP and MEHP (Table I) might be due to inhibition in the electron transport chain. A partial reaction of succinate respiration is electron transfer from succinate to cytochrome *c*. The activity of this segment of the electron transport chain was measured to localize the site of inhibition of succinate oxidation. Succinate cytochrome *c* reductase activity was determined with osmotically lysed mitochondria in order to eliminate the carrier-mediated transport of succinate